frontiers in Mechanical Engineering

REVIEW
published: 18 September 2019
doi: 10.3389/fmech.2019.00049

Review of the Transition From Smouldering to Flaming Combustion in Wildfires

Muhammad A. Santoso[1], *Eirik G. Christensen*[1], *Jiuling Yang*[2] *and Guillermo Rein*[1]*

[1] Department of Mechanical Engineering, Imperial College London, London, United Kingdom, [2] State Key Laboratory of Fire Science, University of Science and Technology of China, Hefei, China

Wildfires are uncontrolled combustion events occurring in the natural environment (forest, grassland, or peatland). The frequency and size of these fires are expected to increase globally due to changes in climate, land use, and population movements, posing a significant threat to people, property, resources, and the environment. Wildfires can be broadly divided into two types: smouldering (heterogeneous combustion) and flaming (homogeneous combustion). Both are important in wildfires, and despite being fundamentally different, one can lead to the other. The smouldering-to-flaming (StF) transition is a quick initiation of homogeneous gas-phase ignition preceded by smouldering combustion, and is considered a threat because the following sudden increase in spread rate, power, and hazard. StF transition needs sufficient oxygen supply, heat generation, and pyrolysis gases. The unpredictable nature of the StF transition, both temporally and spatially, poses a challenge in wildfire prevention and mitigation. For example, a flaming fire may rekindle through the StF transition of an undetected smouldering fire or glowing embers. The current understanding of the mechanisms leading to the transition is poor and mostly limited to experiments with samples smaller than 1.2 m. Broadly, the literature has identified the two variables that govern this transition, i.e., oxygen supply and heat flux. Wind has competing effects by increasing the oxygen supply, but simultaneously increasing cooling. The permeability of a fuel and its ability to remain consolidated during burning has also been found to influence the transition. Permeability controls oxygen penetration into the fuel, and consolidation allows the formation of internal pores where StF can take place. Considering the high complexity of the StF transition problem, more studies are needed on different types of fuel, especially on wildland fuels because most studied materials are synthetic polymers. This paper synthesises the research, presents the various StF transition characteristics already in the literature, and identifies specific topics in need of further research.

Keywords: fire, forest, flame, wildland urban interface, polymer

OPEN ACCESS

Edited by:
Michael John Gollner, University of Maryland, College Park, United States

Reviewed by:
Sara McAllister, Rocky Mountain Research Station, United States Forest Service, United States
Chris Lautenberger, California Polytechnic State University, United States

***Correspondence:**
Guillermo Rein
g.rein@imperial.ac.uk

Specialty section:
This article was submitted to Thermal and Mass Transport, a section of the journal Frontiers in Mechanical Engineering

Received: *26 February 2019*
Accepted: *24 July 2019*
Published: *18 September 2019*

Citation:
Santoso MA, Christensen EG, Yang J and Rein G (2019) Review of the Transition From Smouldering to Flaming Combustion in Wildfires. Front. Mech. Eng. 5:49. doi: 10.3389/fmech.2019.00049

INTRODUCTION TO SMOULDERING COMBUSTION

Smouldering combustion is the slow, low-temperature, flameless burning of porous fuels, and the most persistent type of combustion phenomena (Rein, 2016). A wide range of materials can undergo smouldering, such as cellulosic insulation, coal, polyurethane (PU) foam, cotton, wood, and peat, making smouldering a serious hazard in both residential and wildland areas. In particular,

TABLE 1 | Smouldering and flaming combustion characteristics (Hadden et al., 2014; Rein, 2016).

Characteristics	Smouldering	Flaming
Peak temperature [°C]	450–700	1,500–1,800
Typical spread rate [mm/min]	1	100
Effective heat of combustion [kJ/kg]	6–12	16–30
Ignition source [kW/m^2]	8	30

the hazard of wildfire increases at the wildland urban interface (WUI), where wildfire fronts meet houses and urban sites. In such an event, two types of fuels are involved, i.e. WUI and wildland fuels. WUI fuels are found in the built environment (e.g., polymers and timber), where the smouldering-to-flaming (StF) transition has been investigated in more studies than wildland fuels (e.g., leaves, twigs, and organic soils), which are rarely discussed in the literature. In any fuel, both smouldering and flaming can occur, and one can lead to the other (Rein, 2016).

The chemical pathways of solid fuel combustion can be broadly simplified to the following equations (Equations 1–3). Notably, smouldering (Equation 2) and flaming (Equation 3) fires of solid fuel. Although flaming is characterisitically different from smouldering; smouldering is the heterogeneous reaction of solid fuel with an oxidiser, whereas flaming is the homogeneous reaction of gaseous fuel with an oxidiser, which releases more heat (**Table 1**); the two fires have their genesis from the same process, namely, pyrolysis (Equation 1).

Pyrolysis:

$$\textit{Fuel}\ (\textit{solid}) + \textit{Heat} \rightarrow \textit{Pyrolyzate}\ (\textit{gas}) + \textit{Char}\ (\textit{solid}) + \textit{Ash}\ (\textit{solid}) \quad (1)$$

Heterogeneous oxidation (smouldering):

$$\textit{Char}\ (\textit{solid}) + O_2\ (\textit{gas}) \rightarrow \textit{Heat} + CO_2 + H_2O + \textit{other gases} + \textit{Ash}\ (\textit{solid}) \quad (2)$$

Gas-phase oxidation (flaming):

$$\textit{Pyrolyzate}\ (\textit{gas}) + O_2\ (\textit{gas}) \rightarrow \textit{Heat} + CO_2 + H_2O + \textit{other gases} \quad (3)$$

The commonality of pyrolysis (Equation 1) prior to both smouldering and flaming combustion allows the transition between them. In one case, a flaming fire can extinguish, and a smouldering fire can proceed in a flaming-to-smouldering transition. This transition may have significant effects on soil consumption during wildfires, as flaming fires quickly spread over the surface of the forest floor and consume shallow layers of ground fuels, while smouldering occurs both above- and belowground, slowly releasing vast amounts of carbon, and is far more detrimental to the ecosystem. For example, during peat fires in Indonesia in 1997, it was found that smouldering combustion consumed organic soils as deep as 51 ± 5 cm and released approximately 2.57 Gt of carbon (Page et al., 2002). At the global scale estimate, the average annual greenhouse gas emissions from smouldering fires are equivalent to 15% of man-made emissions (Rein, 2013). Owing to its low temperature, propensity to travel belowground, and flameless characteristics, smouldering of organic soils is difficult to detect (Page et al., 2002; Rein et al., 2008; Rein, 2016). Additionally, when detected, smouldering is notoriously difficult to extinguish, requiring vastly greater quantities of water (Hadden and Rein, 2011; Rein, 2016; Ramadhan et al., 2017; Ratnasari et al., 2018).

In Southeast Asia, this flaming-to-smouldering transition is common, as it is frequently used in agricultural practices to clean the land and return nutrients for use in plantations—this practice is typically referred to as slash and burn (**Figure 1**). These practices can lead to widespread peat fires during prolonged dry spells, such as El Nino, and are often the cause of dramatic haze episodes, such as those regularly recorded in Indonesia (Page et al., 2002; Huijnen et al., 2016). Additionally, smouldering wildfire produces more toxic compounds per kilogram of fuel compounds than flaming (Rein, 2016; Hu et al., 2019), and due to the low temperature causing weakly buoyant plumes, smoke can be blown into nearby cities, causing severe degradation of air quality and significant adverse health effects (World Health Organization, 2006; Rein, 2016; Hu et al., 2018). In 2015, the haze episode caused an economic loss of 16 billion US$ to Indonesia, not including economic losses to the other affected countries, such as Malaysia, Singapore, and Brunei Darussalam[1].

However, the more dramatic transition is StF, as it represents a sudden increase in spread rate, power, and hazard (**Table 1**). Smouldering ignition requires less energy than flaming ignition, and as such, the StF transition provides a path to flaming *via* heat sources too weak to directly ignite a flame (Hadden et al., 2014). In addition, based on the review of research of fire spread in WUI fires, Caton et al. (2017) identify StF transition as one of the pathways of building fire spread in the WUI fires. There is a rather informal technical term used to express the reignition of fire that previously has been extinguished, i.e., rekindle (NWCG, 2012). StF transition can be one of the mechanisms leading to rekindling in wildfire. This is further discussed in the section *Embers and StF Transition in Wildfires*.

In addition to heat flux from the flame, embers generated by wildfires are a major cause of wildfires spread and ignition in WUI building (Mell et al., 2010). Embers (also called as firebrands or firedrops) are pieces of hot or burning fuel lofted by the plume of the fire (Fernandez-Pello, 2017) (**Figure 2**). Once accumulated, embers can cause WUI structures such as roofing material, decks, and vents to smolder and, in some cases, transition to flaming. The generation of embers, its transport and the vulnerability of ignition of WUI fuels due to flaming and smouldering embers have been widely investigated (Manzello et al., 2008, 2009, 2012, 2017; Manzello, 2014; Manzello and Suzuki, 2014, 2017; Suzuki et al., 2015; Zhou et al., 2015; Hakes et al., 2018). Embers also provide an alternative mode of fire spread during wildfires through spotting, whereby embers land and locally ignite dry fuels, often transitioning from StF and thus

[1]Haze fires cost Indonesia S$ 22 b, twice the tsunami bill: World Bank, *The Straits Times*, Singapore, 16 December 2015.

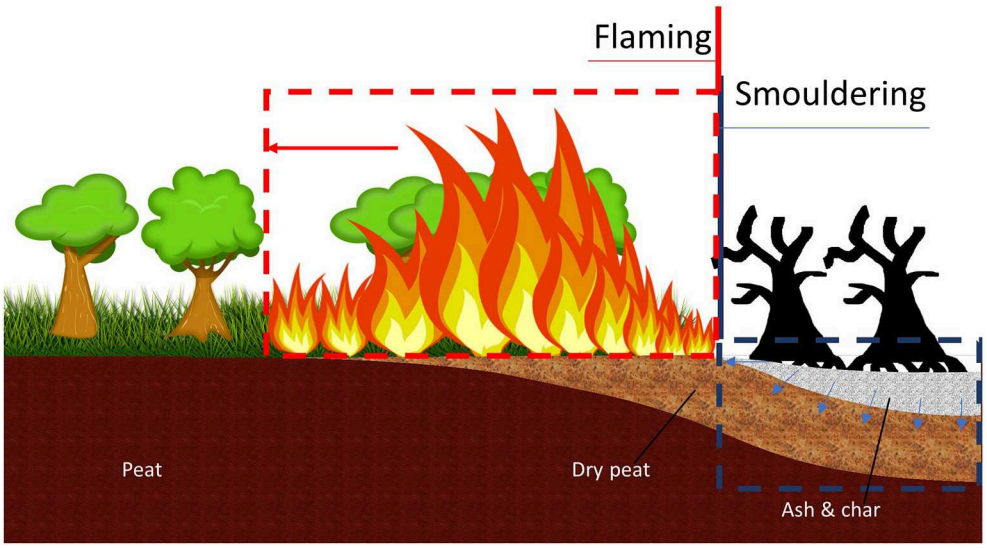

FIGURE 1 | Simultaneous occurrence of smouldering and flaming in peatland forest fires. Flaming wildfire consumes surface fuel vegetation and tree crowns. Smouldering combustion consumes organic soil, dominantly spreading on and below the ground.

advancing the flame (**Figure 2**). This particular behaviour can be highly hazardous to firefighters who may quickly find themselves surrounded by flames. Moreover, the current codes and standards of WUI represent a lack of understanding of how WUI structure can ignite during wildfire, one of which is the WUI structural vulnerability to ember showers (Manzello and Quarles, 2017; Manzello et al., 2018).

Despite the significant risks associated with the transition from StF, limited research is available on the topic, and a fundamental theory of the phenomena has yet to be found. Current research has identified a few key mechanisms but has also found that the transition is inherently difficult to predict. This unpredictable nature of the StF transition both temporally and spatially poses an additional challenge in wildfire prevention and mitigation. This paper aims to synthesise findings in the literature of the StF transition and identify the leading mechanisms and key influencing variables for both wildland and WUI fuels to identify further research required to fully understand the StF transition.

FIGURE 2 | Ember shower during the 2018 Delta Fire in the Shasta-Trinity National Forest, California, USA. Photo courtesy of Noah Berger/Associated Press (noahbergerphoto.com). Photo shows flaming fires of grass due to embers, representing a smouldering-to-flaming transition from embers.

ROLE OF OXYGEN SUPPLY AND HEAT TRANSFER

Airflow has been frequently found to be a factor that influences the StF transition, as it increases the oxygen supply into the reaction zone, increasing the smouldering spread rate. The StF transition is likely to occur with increasing smouldering spread rate as the intensity of combustion and rate of pyrolysis increase, resulting in a greater mass flux of pyrolyzates. Palmer (1957) particularly described that the StF transition was preceded by glowing, which is the visual indication of a high local temperature due to strong smouldering (Rein, 2016). Notably, the wind direction relative to the spread is also markedly important to the spread dynamics of smouldering. Forward smouldering propagates in the same direction as the airflow, whereas opposed smouldering propagates against the flow of air (Rein, 2016). Forward and opposed smouldering propagations represent different heat transfer mechanisms that influence the heating process of the fuel (Ohlemiller, 1985; Rein et al., 2007; Rein, 2009, 2016), thus affecting the occurrence of the StF transition. In opposed smouldering, airflow carries the heat from the smouldering zone away to the ash layer, diminishing the heat supplied for heating the fuel. In forward smouldering, the airflow transfers heat from the smouldering zone to the unreacted fuel, resulting in a

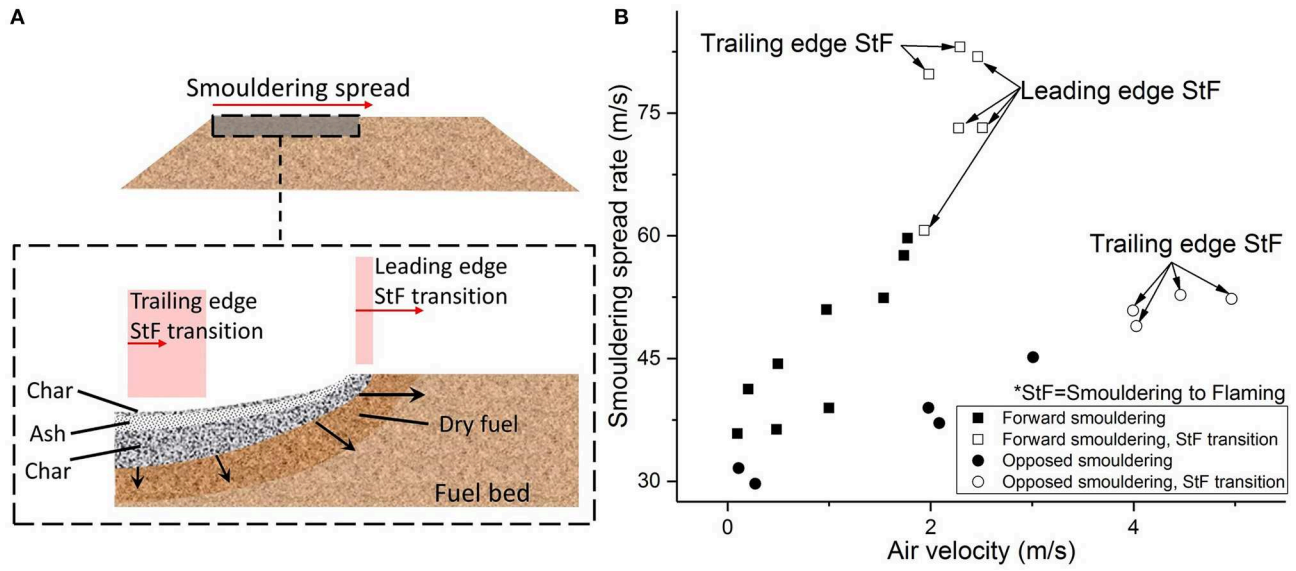

FIGURE 3 | (A) Smouldering front diagram showing leading and trailing edges of the StF transition. No significant smouldering front structures between forward and opposed smouldering in Ohlemiller (1990) other than the relative thickness of each layer, i.e., drying, char, and ash layers. The detailed smouldering front diagram is a modification from X. Huang (CC BY license) in Huang and Rein (2014). The shaded red area represents the rough estimation of the possible location for the StF transition. Red arrow indicates the duration length of the StF transition. **(B)** Smouldering spread rate of cellulosic insulation under forward and opposed smouldering propagation modes. Data from Ohlemiller (1990).

more efficient fuel heating process. The smouldering front is also narrower in opposed smouldering than in forward smouldering, representing the lower amount of heat produced in opposed smouldering (Rein et al., 2007). Due to the stronger influence of airflow on the smouldering spread rate in forward smouldering than in opposed smouldering, forward smouldering has a greater propensity for the StF transition (Palmer, 1957; Chen et al., 1990; Ohlemiller, 1990).

StF transitions can also occur under opposed smouldering (Ohlemiller, 1990, 1991; Aldushin et al., 2009) but with a lower propensity than those under forward smouldering because of the heat transfer direction discussed previously. Basically, the increase in airflow velocity plays two roles in smouldering. Airflow increases both oxygen supply to the smouldering front and convective heat loss. Increased oxygen supply increases the rate of the exothermic reaction needed to sustain smouldering, while increased convective heat losses decrease heat transfer into the unreacted fuel. The latter role is more significant in opposed smouldering propagation than in forward smouldering propagation.

Two types of StF transitions were identified by Ohlemiller (1990): trailing- and leading-edge transitions (**Figure 3A**). **Figure 3A** illustrates smouldering fronts and the location of the leading-edge and trailing-edge StF transitions. The trailing-edge StF transition occurred at the char layer at the trailing edge of the smouldering front. The flame caused by this transition was blue, lasted up to 2 min, and spread up to 10 cm on the residual char. The blue color of the flame was probably due to a lean mix of gaseous fuel with air prior to ignition. In addition to the mixture concentration, the fuel (i.e., hydrocarbon such as CO or pyrolyzate Ohlemiller, 1990) is known to affect the color of the flame, along with the tendency to produce soot. The leading-edge StF transition occurred at the leading edge of the smouldering front, spread downstream onto the unburnt layer of cellulosic insulation, and lasted up to 5 min. **Figure 3B** shows that both leading-edge and trailing-edge StF transitions occurred in forward smouldering, while only the trailing-edge StF transition occurred in opposed smouldering under an airflow of up to 5 m/s. Considering the slower smouldering spread in opposed smouldering, it can be seen that a slower smouldering spread rate results in a lower StF transition propensity.

Building on this fundamental concept of the rate of oxidation being crucial in the transition phenomena, the increase in ambient oxygen concentration has been investigated and found to have a profound effect on the StF transition. StF transitions of smouldering PU foam with no external airflow occurred at oxygen concentrations ranging from 17 to 37 vol%, depending on the ambient pressure, and only for large samples (50 × 120 × 450 mm; Ortiz-Molina et al., 1979). The samples in the form of small cylinders (18 mm in diameter) did not experience a transition. The dimensions of the sample govern the self-sustainability of smouldering since smaller samples lead to higher heat losses (Torero and Fernandez-Pello, 1995). By increasing ambient pressure, the oxygen concentration at which the StF transition occurred (critical oxygen concentration) decreased. This result implies that increased oxygen diffusion penetration into smouldering fuel under increased ambient pressure leads to lower critical oxygen concentration. However, when the ambient oxygen concentration is further increased to 35–54 vol% with assistive heating (4.5–55 kW/m^2), the StF transition can occur in

samples with characteristic lengths as small as 10–12.5 cm (Sato and Sega, 1991; Bilbao et al., 2001; Bar-Ilan et al., 2005; Putzeys et al., 2006, 2007, 2008).

It is important to note that in wildfires, the oxygen concentration will not become higher than the atmospheric oxygen concentration. In fact, the oxygen concentration can be lower. Thus, the effect of airflow velocity and particle diameter in terms of oxygen supply is the most prominent in the StF transition in wildfires. Other important parameters in wildland fuel are moisture content (MC) and inorganic content (IC). MC and IC reduce the propensity to ignition and decrease the lateral fire spread rate of wildland fuel due to their roles as heat sinks (Frandsen, 1987, 1997; Huang et al., 2016; Rein, 2016; Christensen et al., 2019; Santoso et al., 2019). MC absorbs heat for water vaporisation, and IC absorbs heat and does not contribute to further exothermic reactions due to its inert nature, contributing to increased heat losses. Interestingly, it has been recently reported that the in-depth spread rate increases with MC, which is counterintuitive to the widely assumed decrease in spread rate with MC (Huang and Rein, 2017). Thus, the lateral and in-depth spread rates in smouldering fires respond differently to MC. As MC increases, the density of organic matter per unit volume decreases and porosity increases due to volumetric expansion. The spread rates, i.e., lateral and in-depth, are limited and pre-dominantly governed by two different processes of heat loss and oxygen diffusion. However, the mechanism causing these different responses still needs further investigation. Increased propensity of the StF transition with decreased MC has been shown in both WUI and wildland fuels (Chao and Wang, 2001; Manzello et al., 2006a,b; Wang et al., 2017).

The critical velocity of the StF transition occurred as the velocity ranged from 1 to 5 m/s for studies at atmospheric oxygen concentration and without assistive heating, such as radiant heating, deposited embers, and deposited hot particle (**Table 2**). With external heat flux and increased ambient oxygen concentration, the critical velocity decreased because the convective cooling effect was minimised (Bar-Ilan et al., 2005). In turn, the decreasing convective cooling effect decreased the required heat needed to induce the StF transition. In the case of the deposition of embers at atmospheric oxygen concentration, the StF transition was found to occur at velocities as low as 1 m/s (Manzello et al., 2006a,b) or even with no airflow velocity when the assistive heating was from a hot steel particle at a temperature of ∼1,200°C (Wang et al., 2017).

In all investigated consolidated WUI fuels (**Table 2**), the StF transition occurred only if the smouldering sample was assisted with heat insulation, heated boundaries, and increased ambient oxygen concentration (Ortiz-Molina et al., 1979; Tse et al., 1996; Bar-Ilan et al., 2005; Putzeys et al., 2006, 2007, 2008; Chang et al., 2011). However, this finding is not the case when there is a radiation exchange between smouldering char surfaces (Alexopoulos and Drysdale, 1988; Ohlemiller, 1991; Stoliarov et al., 2017). In this case, the critical airflow velocity of the StF transition can be lower than 1 m/s, even without assistive external heating and elevated ambient oxygen concentration. Ohlemiller (1991) found that the StF transition consistently occurred in both forward and opposed smouldering for airflows between 0.2 and 0.25 m/s with a smouldering sample in a U-shaped geometry. The U-shaped geometry increased the radiation heat exchange between the smouldering surfaces of a wood sample. The increased radiation exchange is also the prominent factor in the StF transition mechanism hypothesised from a series of upholstered furniture fire tests (Babrauskas and Krasny, 1985, 1997; Ogle and Schumacher, 1998), as discussed further in the next section.

THE CHIMNEY EFFECT

Many StF transition investigations, especially for upholstered furniture, were conducted during the 1970s and 1980s due to the concern of residential fires in which cigarettes were considered to be the major cause of ignition (Clarke and Ottoson, 1976; Babrauskas and Krasny, 1985). From a series of tests with assorted sofas, chairs, mattresses, and box springs as test materials, the time to StF transition occurred from 20 to 132 min (Clarke and Ottoson, 1976; Bukowski et al., 1977; Harpe et al., 1977; Bukowski, 1979). It was not until the fire tests conducted by Ogle and Schumacher (1998) that the mechanism leading to the StF transition was proposed. The proposed mechanism emphasised the role of oxygen supply and air current in inducing the StF transition. Ogle and Schumacher (1998) performed 11 fire tests on 10 upholstered furniture items, where seven tests were ignited by a smouldering cigarette and four using a flaming liquid fuel. The StF transition was preceded by a "burn-through" of the smouldering cigarette at a crevice location of upholstered furniture (**Figure 4**). This "burn-through" is downward smouldering cigarette propagation through the crevice of cushions forming a narrow vertical channel due to smouldering consumption of the cushion material. The formation of this narrow vertical channel enhances the air entrainment to the smouldering zone from below due to the chimney effect. The greater air entrainment increases both oxygen supply to smouldering reaction and convective heat losses. However, the convective heat losses are compensated for by the radiation exchange between the two smouldering surfaces facing each other, which are also more exothermic due to the enhancement air entrainment. This leads to vigorous smouldering which is favourable for the StF transition.

The radiation exchange between the two smouldering char surfaces in a vertical channel influences the StF transition and induces a StF transition even at low airflow velocities, i.e., 0.1–0.27 m/s (Alexopoulos and Drysdale, 1988; Ohlemiller, 1991). In experiments of chimneys with different shapes, i.e., square, rectangular, and slot shaped, conducted by Alexopoulos and Drysdale (1988) (**Figure 5A**), the time to StF transition was found to be independent of airflow and shortest in the chimney shape with the narrowest vertical channel space, i.e. the slot-shaped chimney (**Figure 5B**). The temperatures inside the vertical channel, i.e., T_1 and T_2 (**Figure 5A**), were higher in the slot-shaped chimney than in the square and rectangular chimneys. This temperature trend and independence of the StF transition time to airflow imply that conservation of heat governs the StF transition mechanism along with oxygen supply. This

TABLE 2 | Studies of the smouldering-to-flaming transition in the literature.

Consolidation/ fuel category	Sample material	Sample shape and orientation (characteristic length [m])	Ignition source (size and duration)	smouldering spread mode	Critical velocity [m/s]	Oxygen concentration [vol%]		External heat flux [kW/m^2]		Location of transition	Time to StF transition [mm:ss]	References
						Experiment range	Critical	Experiment range	Critical			
Unconsolidated/ Wildland fuel	Pine straw mulch, Shredded hardwood mulch, Cut grass, Pine needles	Thin rectangular block/horizontal (0.23)	smouldering embers [four 50 mm (diam.) by 6 mm (thick), 1.5 g]	Forward and opposed (simultaneously)	1	21	21	N/A (ember)	N/A (ember)	Free surface	N/A	Manzello et al., 2006a and Manzello et al., 2006b
	Pine needles	Thin rectangular block/horizontal (0.31)	Spherical metal particle (Diam. 6, 8, 10, 12, 14 mm and temperature 680–1,190°C)	Forward	0–4	21	21	None	From the hot steel particle under high temperatures	Free surface	~01:40–10:20	Wang et al., 2017
	Pine needles	Thin rectangular block/horizontal (0.6)	Flaming wood stick (4 × 4 × 130 mm) on dry pine needle bed (150 × 20 × 40 mm)	Forward	1.1	21	21	None	None	Free surface	N/A	Valdivieso and Rivera, 2014
Unconsolidated/ WUI fuel	Filter paper and cardboard	Cylindrical/vertical (0.1)[#1]	Small flame (N/A)	Opposed	1.52 ± 0.82 (Filter paper) 1.73 ± 0.81 (Cardboard)	18–62	52 ± 2 (Filter paper) 44 ± 4 (Cardboard)	N/A	N/A	N/A	N/A	Sato and Sega, 1991
	Cork dust and deal sawdust[¶]	Rectangular block/horizontal (0.15–0.2)	Small flame (N/A)	Forward	1.8 ± 0.8	21	21	N/A	N/A	Free surface	N/A	Palmer, 1957
	Cellulosic insulation	Flat rectangular with wedge ends/horizontal (0.46)	Electrical heater (375°C and 60 min)	Forward and opposed	2.2 ± 0.22 (forward) 4.4 ± 0.4 (opposed)	21	21	N/A	N/A	Free surface	N/A (50:00[I])	Ohlemiller, 1990
	Wood shavings, shredded papers, beeswings*	Rectangular block/horizontal (0.61)[#2]	Electrical coil (80 V and N/A)	Forward and opposed (simultaneously)	2.23 ± 0.63 (wood shaving) 0 (Shredded paper)	21	21	N/A	N/A	N/A	02:00–76:00	Chen et al., 1990

(Continued)

TABLE 2 | Continued

Consolidation/ fuel category	Sample material	Sample shape and orientation (characteristic length [m])	Ignition source (size and duration)	smouldering spread mode	Critical velocity [m/s]	Oxygen concentration [vol%]		External heat flux [kW/m^2]		Location of transition	Time to StF transition [mm:ss]	References
						Experiment range	Critical	Experiment range	Critical			
Consolidated/ WUI fuel	*Pinus pinaster*	Thin slab/horizontal (0.11)	Spontaneous, Propane-air flame (piloted, no airflow, 10 mm flame length), Electrical spark (piloted, with airflow)	N/A	2.4 ± 1.4	21	21	10–55	35.48 ± 9.61	N/A	00:09–12:17 (spontaneous) 00:10–13:10 (Piloted)	Bilbao et al., 2001
	Fiber-insulated board	Hollow rectangular block/ vertical (0.15)	Bunsen flame	Forward	0.18 ± 0.06	21	21	N/A	N/A	Free surface	10:12–23:36	Alexopoulos and Drysdale, 1988
	Fire-retarded (FR) and Non-fire-retarded (NFR) polyurethane (PU) foam	Rectangular block/horizontal (0.1–0.4)	Electrical heater (40–200 W)	Lateral in natural convection	N/A	21	21	N/A	N/A	Free surface	60:00–138:05	Chao and Wang, 2001
	NFR PU foam	Rectangular block/vertical (0.125)	Electrical heater (23.25 W and until self-sustained smouldering identified)	Forward	0.82 ± 0.5	30–40	37.5 ± 2	7.25–8.75	8 ± 0.6	Within the sample	17:34	Bar-Ilan et al., 2005
	FR PU foam	Rectangular block/vertical (0.125)	Electrical heater (115 W and 250–300 s)	Forward	0.15	30–60	42.5 ± 7.5	4.5 or 5.5	5 ± 0.5	Within the sample	09:12	Putzeys et al., 2006
	NFR PU foam	Rectangular block/vertical (0.125)	Electrical heater (23.25 W and 11.7 min)	Forward	0.5	25 and 40	35 and 40	8 and 8.75	8 and 8.75	Within the sample	17:00 (∼16:00‡)	Putzeys et al., 2007
	PU foam (NFR and FR)	Rectangular block/vertical (0.125)	smouldering: electrical heater (23 W for NFR foam and 115 W for FR foam)	Forward	0.5 (NFR)	15–35	0.2 ± 0.02 (NFR foam)	7.25–8.75 (NFR)	5 ± 0.5 (NFR foam)	Within the sample	∼18:00 (NFR foam at 21 vol% O_2 and 8 kW/m^2)	Putzeys et al., 2008
			Pilot ignition: resistance wire (8.8 A for NFR foam and 10 A for FR foam)		0.15 (FR)		0.28 ± 0.05 (FR foam)	4.5 and 5.5 (FR)	8 ± 0.61 (FR foam)			

(Continued)

TABLE 2 | Continued

Consolidation/ fuel category	Sample material	Sample shape and orientation (characteristic length [m])	Ignition source (size and duration)	smouldering spread mode	Critical velocity [m/s]	Oxygen concentration [vol%]		External heat flux [kW/m^2]		Location of transition	Time to StF transition [mm:ss]	References
						Experiment range	Critical	Experiment range	Critical			
	NFR PU foam	Rectangular block/horizontal (0.23)[#3]	Cigarette ignition	Lateral in natural convection	N/A	21	21	None	None	N/A	~50:00	Chang et al., 2011
	NFR PU foam lined with cotton fabric	Rectangular block/vertical (0.3)	Electrical heater rod (Diam. 0.64 cm, 11 W DC)	Upward natural convection	N/A	21	21	None	None	Free surface	14:00–60:00	Stoliarov et al., 2017
	NFR PU foam	Rectangular block/vertical (0.381)	Electrical heater (70 W and 50 min)	Forward	0.78 ± 0.48	21	21	N/A	N/A	Within the sample	56:54–127:36	Tse et al., 1996
	NFR PU foam	Rectangular block/vertical (0.406)	Electrical heater (70 W and 50 min)	Forward	0.25 and 0.75	21	21	N/A	N/A	Within the sample	96:00–113:00	Tse et al., 1996
	NFR PU foam	Rectangular block/horizontal (0.45)	Heating element (N/A)	Lateral in natural convection	N/A	17–62	27.7 ± 8.1	N/A	N/A	N/A	N/A	Ortiz-Molina et al., 1979
	Red oak and White pine	U-shaped rectangular block/horizontal (0.74)	Electrical heater (N/A and 60 min)	Forward, opposed, and mixed	0.23 ± 0.03	21	21	N/A	N/A	Free surface	N/A	Ohlemiller, 1991
	Upholstered furniture	Upholstered shapes and orientations (N/A)	Cigarette and electrical ignition (N/A)	N/A	N/A	21	21	N/A	N/A	In the crevice between two cushions	18:00–306:00	Babrauskas and Krasny, 1985, 1997; Ogle and Schumacher, 1998
	Cedar, Douglas-fir, Redwood	Slab/horizontal (1.2)	Firebrand showers (17.1 ± 1.7 g/m^{2}s)	Forward and opposed (simultaneously)	6	21	21	N/A [ember(s) shower]	N/A [ember(s) shower]	Free surface	05:56–19:40	Manzello and Suzuki, 2014
	Oriented strand board (OSB); roofing assembly (OSB, tar paper, and shingles); and dried pine needles and leaves	Valley configuration of OSB; and flat configuration of roofing assembly with attached gutter filled by dried pine needles and leaves/angled position (1.22)	Firebrand showers (up to 0.4 g and 6 min)	Forward and opposed (simultaneously)	7	21	21	N/A [ember(s) shower]	N/A [ember(s) shower]	In the crevice[§] and in the gutter[8]	N/A	Manzello et al., 2008

(Continued)

TABLE 2 | Continued

Consolidation/ fuel category	Sample material	Sample shape and orientation (characteristic length [m])	Ignition source (size and duration)	smouldering spread mode	Critical velocity [m/s]	Oxygen concentration [vol%]		External heat flux [kW/m^2]		Location of transition	Time to StF transition [mm:ss]	References
						Experiment range	Critical	Experiment range	Critical			
	Cotton	Cuboid/vertical (0.15)	Electrical heater (12.8 kW/m^2 and 24 min)	Upward natural convection[#4]	N/A	21	21	None	None	Within the sample	117:00, 118:00, 133:00	Hagen et al., 2015
	OSB	Slab/horizontal (0.18)	Fire brand [L 25.4 × Ø 6.35, 9.52, 12.7 mm × piles (1 brand, 20, 50, and 100 g)]	Forward and opposed (simultaneously)	1.84	21	21	N/A [ember(s) deposition]	N/A [ember(s) deposition]	Free surface	∼01:30	Hakes et al., 2018

In some studies, the ignition source also acted as the continuous external heat flux to the sample, i.e., ember accumulation on fuel sample.

[¶]*No transition to flaming in samples with particle diameters <0.1 cm.*

[I]*Computationally predicted by Yang et al. (2018).*

[†]*Computationally predicted by Dodd et al. (2012).*

[*]*Transition to flaming only occurred once in thin filmy pieces of bran.*

[§]*For material construction of valley configuration with only base material (oriented strand board).*

[8]*For the flat configuration of roofing assembly attached with gutters filled by dried pine needles and leaves.*

[#1]*Diameter varied from 0.0027 to 0.0054 m.*

[#2]*Depth varied from 0.1 to 0.2 m.*

[#3]*Width varied from 0.08 to 0.16 m.*

[#4]*Sample was in a cube shape and ignited at the bottom.*

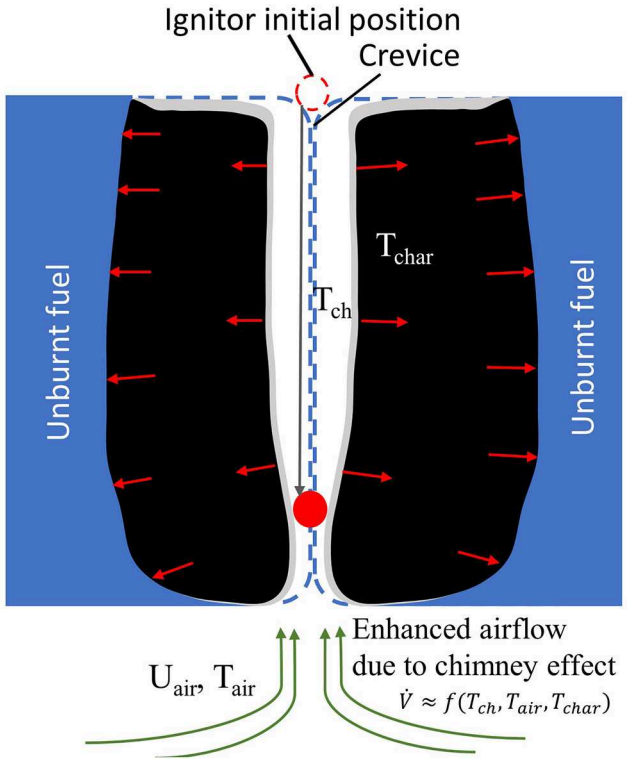

FIGURE 4 | Enhanced oxygen supply in the channel formed by downward smouldering propagation of an ignitor at the crevice location of two adjacent solid fuels. The enhanced airflow increases the oxygen supply to the smouldering fuel, leading to a more exothermic smouldering reaction. This figure is an adaptation from Ogle and Schumacher (1998).

result is in agreement with recent findings by Stoliarov et al. (2017), who performed a series of experiments of smouldering PU foam under natural convection with an adjustable vertical channel gap between the front face of the PU foam and a thermal insulation plate (**Figure 6A**). With a large gap, the oxygen supply was adequate, and smouldering was the dominant reaction (**Figure 6B**). With a smaller gap, smouldering was not the dominant reaction due to insufficient oxygen supply (**Figure 6C**). With the availability of heat from smouldering and a deficient oxygen supply, pyrolysis was more intense in the smaller gap configuration than in the larger channel gap configuration, leading to more pyrolyzates being produced. Moreover, a smaller gap might result in a higher concentration of pyrolyzates inside the channel (**Figure 6B**). The StF transition then occurred when the pyrolyzates were heated by char oxidation up to the point where the pyrolyzate temperature and concentration were above the lower flammability limit. In this case, the StF transition was a piloted ignition of pyrolyzate by char oxidation. This finding was also observed by Alexopoulos and Drysdale (1988), who found that the StF transition time was longer in wider vertical channel gaps. In another study of StF transitions in small *Pinus pinaster* wood samples with dimensions of 11 by 11 by 1.9 cm, Bilbao et al. (2001) found that the radiative heat flux affected the time to StF transition more than convection. A previous ignition study of polyurethane foam found that the critical radiation heat flux to ignite smouldering is lower than that to ignite flaming combustion and decreases with sample size (Hadden et al., 2014). This result represents the important role of radiation heat transfer in smouldering and the following possible StF transition.

The mechanism of the StF transition at a crevice location is particularly important in WUI fires, i.e., where two or more fuels abut each other such as in wood decks and house roofing. The deposition of embers in a crevice of these fuels has been experimentally investigated as a favourable location for ember accumulation that leads to a StF transition (Manzello et al., 2008; Manzello and Suzuki, 2014). Fundamentally, this follows the same mechanism as that shown in **Figure 4**. In addition, wood was found to crack during smouldering. This cracking leads to local crevice formation on the wood surface, leading to a StF transition without heating support from embers (Ohlemiller, 1991).

SECONDARY CHAR OXIDATION

The mechanism of the StF transition due to strong secondary char oxidation (SCO) was first proposed by Torero and Fernandez-Pello (1995), who conducted an experimental study of upward smouldering combustion of polyurethane foam in natural convection (**Figure 7A**). In this experiment, the StF transition was preceded by a second oxidation of char, which was more exothermic than the first. This mechanism is best discussed by referring to **Figure 7B**. Upward smouldering propagation was initiated from t_1 to t_2. At time t_2, the ignitor was turned off. By this time, smouldering had propagated up to the P_5 position. Temperatures at P_1 to P_4 can be observed to decrease, with the temperature at P_1 decreasing the most. The smouldering spread rate decreased, as indicated by a slower temperature increase in downstream positions, i.e., P_6 and P_7. P_5 and P_6 reached a plateau of the pyrolysis temperature (T_p) by the time the experiment approached time t_3. Thus, smouldering fronts propagated to these positions. SCO occurred between times t_3 and t_4. In this time period, the large temperature increase at P_1 indicates a strong char oxidation in the char layer upstream of the smouldering fronts, which is the second char oxidation in that layer. Hence, the name secondary char oxidation is assigned to this process.

Extinguishment of char oxidation at P_1 is not observed prior to SCO since temperatures were still relatively high (~500–600°C). However, its rate of exothermic reaction decreased, as indicated by the temperature decreases, most likely because of the absence of heating from the ignitor. It can be hypothesised that as the smouldering leading edge moved downstream to P_6, the smouldering trailing edge was still around P_1. This process resulted in increases in the smouldering front thickness as smouldering propagated. The term SCO then represents a sudden increase in the exothermic reaction rate at the smouldering trailing edge.

Due to oxygen consumption by secondary char oxidation (SCO), the oxygen concentration was depleted and unable to sustain further oxidation. During this time, t_4 to t_5, endothermic pyrolysis reactions induced by heat provided by previous SCO

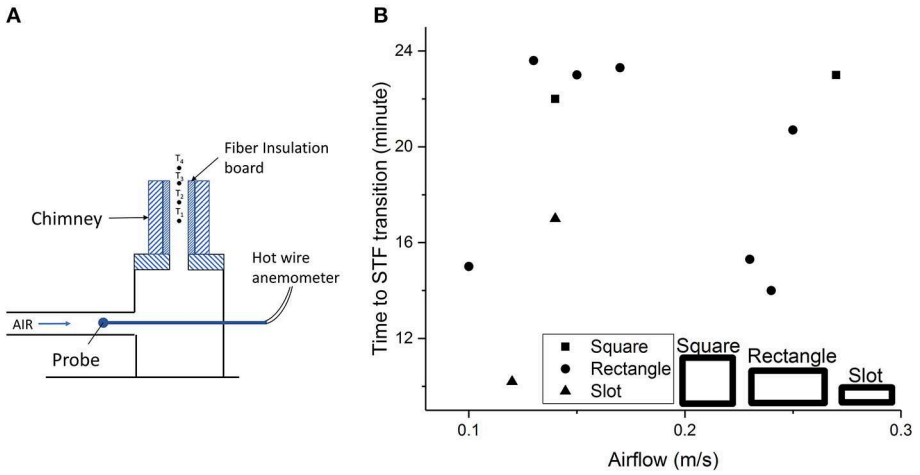

FIGURE 5 | StF transition experiments in a chimney of fiber insulation board (Alexopoulos and Drysdale, 1988). **(A)** Experimental setup of chimney configuration. **(B)** Time to StF transition vs. airflow. Data from Alexopoulos and Drysdale (1988).

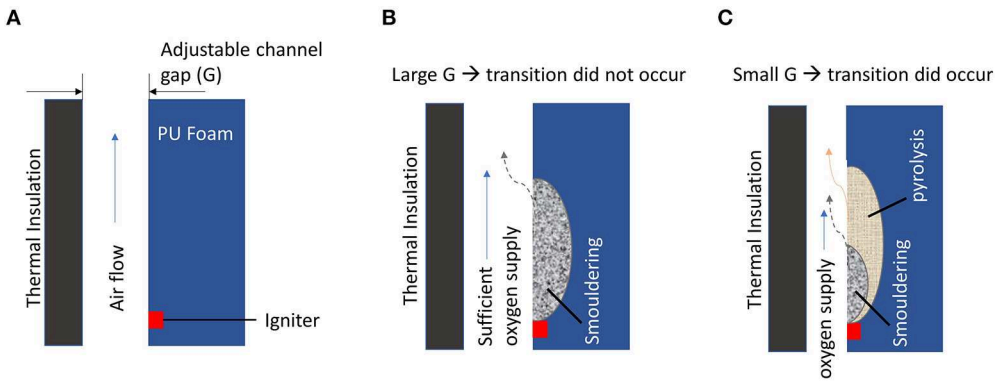

FIGURE 6 | StF transition experiment by Stoliarov et al. (2017). **(A)** Experimental setup. **(B)** Experimental setup in which the StF transition did not occur due to a large channel gap. **(C)** Experimental setup in which the StF transition occurred due to a small channel gap. Solid blue, dotted black, and solid beige arrows indicate oxygen supply, gases and aerosol products from char oxidation, and pyrolyzates, respectively.

took place and produced flammable pyrolyzates, as indicated by the decreasing temperature. Whether char or unreacted PU foam undergoes pyrolysis remains to be determined. Computationally, the pyrolysis of char is one of the key reactions leading to the StF transition (Dodd et al., 2012).

Once the oxygen concentration increased and mixed with the pyrolyzate gases bringin the mixture to within the flammability limits, StF transition occurred (t_5 in **Figure 7B**). This mechanism is consistent with the smouldering of cotton under asymmetric boundary conditions (Hagen et al., 2015). The asymmetric boundary condition was when one face of the cotton sample was closed by a concrete wall. Under this condition, the StF transition occurred due to the slower smouldering spread rate at the closed face than at the open face. One would argue that at the closed face, pyrolysis was more dominant than smouldering due to the insufficient oxygen supply because of the closure by the concrete wall. Pyrolysis provided pyrolyzates that were then ignited by heat provided by smouldering at the open face.

Figure 8A shows a visual observation of the StF transition in a 40-cm-long PU foam slab during upward propagation. In this experiment, one lateral face of the PU foam was exposed to radiant heat flux, the bottom face was in contact with a heater, and the top face as well as the three remaining lateral faces were insulated (Rein, 2009, 2016). Chao and Wang (2001) experimentally investigated the StF transition in PU foam in horizontal propagation under natural convection and found SCO prior to the StF transition. The probability of transition increased with the length of the PU foam.

Recent findings on secondary char oxidation (SCO) were derived from collective works of smouldering PU foam with variable oxidiser supply and radiant heat flux, as shown in **Figure 8B** (Tse et al., 1996; Bar-Ilan et al., 2005; Putzeys et al., 2007, 2008; Dodd et al., 2012). The location of the strong char oxidation upward from the smouldering front, thus located in the char layer upstream of the smouldering leading edge, was confirmed by Tse et al. (1996), who

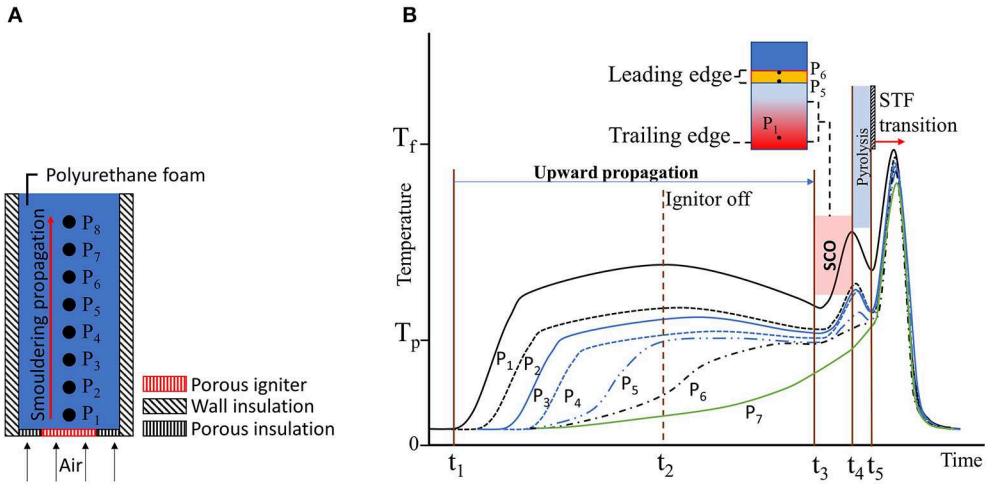

FIGURE 7 | (A) Experimental setup by Torero and Fernandez-Pello (1995). **(B)** Schematic of the temperature distribution in the experiment that led to the StF transition. Figures are redrawn and simplified from the original in Torero and Fernandez-Pello (1995). T_p and T_f are the temperatures at which PU foam undergoes pyrolysis (300°C) and the approximate flaming temperature of PU foam (900–1,000°C).

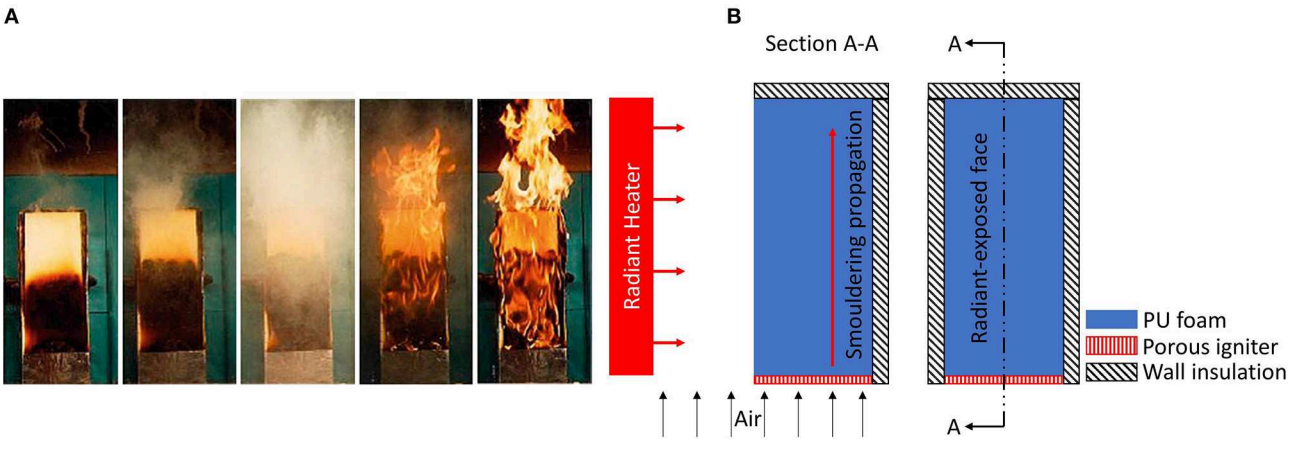

FIGURE 8 | (A) Series of photographs of a combustion experiment illustrating the transition to flaming in a smouldering polyurethane slab 40 cm high under external forced flow (photo by the group of Prof. Carlos Fernandez-Pello, University of California at Berkeley). After 1 h of burning, only half of the sample smouldered (photo 1, far *left*). When the transition took place (photos 2 and 3), the whole sample was engulfed in flames in a few seconds (photos 4 and 5, far *right*). **(B)** Experimental setup of a series of works by Prof. Fernandez-Pello at the University of California at Berkeley, USA (Tse et al., 1996; Bar-Ilan et al., 2005; Putzeys et al., 2007, 2008; Dodd et al., 2012). Figure is redrawn from the original version in Putzeys et al. (2007). Figure on the left shows section A–A cut from the figure on the right.

measured the evolution of permeability inside the PU foam with ultrasonic imaging. The permeability substantially increased as char continued to react. This reaction leads to the formation of voids that provide favourable locations for combustible gas accumulation, thus favouring the StF transition. The SCO, which is more exothermic once reacted, acted as the ignition source for the accumulated gas in the void.

Putzeys et al. (2007) measured the intensity of SCO and concluded that the direction of SCO was downward, while the primary smouldering front was upward. This SCO propagation direction was computationally proven by Dodd et al. (2012), who developed a two-dimensional numerical transport model to predict the StF transition of PU foam in the study by Putzeys et al. (2007). In Dodd et al. (2012) model, there are seven heterogeneous reactions with one global homogeneous gas-phase reaction. Four reactions were important in the model for the StF transition to occur. These reactions are the pyrolysis of thermal char, oxidation of α-char, oxidation of char that produces α-char, and flaming combustion of gaseous fuel. In this scheme, SCO is the oxidation of α-char. The results by Dodd et al. (2012) for temperature and transition time agreed well with the experimental results by Putzeys et al. (2007).

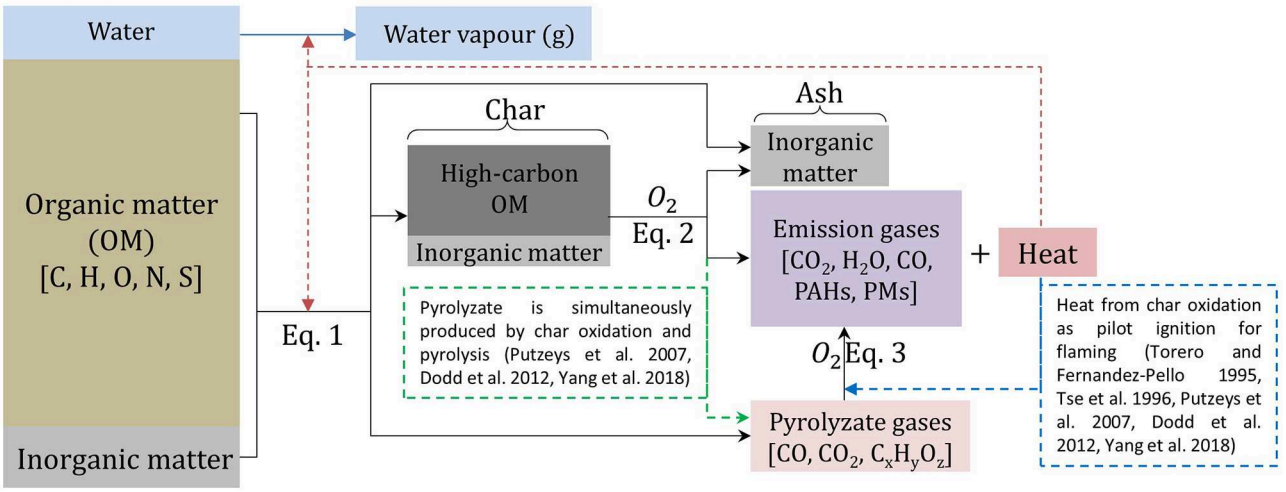

FIGURE 9 | Reaction schematics of organic matter undergoing pyrolysis (Equation 1), smouldering (Equation 2), and flaming (Equation 3). StF transition occurs when oxidation reaction of pyrolyzate (Equation 3) occurs alongside oxidation reaction of char (Equation 2). Solid black lines indicate reaction representing Equations (1–3) in this paper; dotted red line indicates heat feedback from exothermic reaction; blue line indicates evaporation of MC in the fuel; dotted green line indicates pyrolyzate gases production from char oxidation as concluded by Putzeys et al. (2007), Dodd et al. (2012), Yang et al. (2018), and dotted blue line indicates heat feedback from char oxidation that ignite flaming reaction as concluded by Torero and Fernandez-Pello (1995), Tse et al. (1996), Putzeys et al. (2007), Dodd et al. (2012), Yang et al. (2018). Figure after diagram in Lin et al. (2019).

In the kinetic model by Dodd et al. (2012), secondary char oxidation (SCO) is important in providing gaseous fuel and heat required to ignite flaming combustion. This gaseous fuel is produced from SCO and thermal char pyrolysis. Thus, SCO provides gaseous fuel and heat. In addition to sustaining the thermal char pyrolysis which provides the pyrolyzates, heat also acts as the ignitor of the produced gaseous fuel/air mixture once it is above its lower flammability limit. This finding is related to the mechanism proposed by Torero and Fernandez-Pello (1995). To computationally reproduce the experimental work of smouldering cellulosic insulation by Ohlemiller (1990), Yang et al. (2018) found that char oxidation and pyrolysis of cellulose provide gaseous fuel, while the ignitor is the hot char at the surface of the cellulosic insulation (**Figure 9**). There is no SCO in this model. In conclusion, gaseous fuel is simultaneously produced by char oxidation and pyrolysis reaction (**Figure 9**). Whether the prominent pyrolysis reaction takes place on unreacted fuel or char still needs to be determined.

PERMEABILITY AND CONSOLIDATION

Two material properties that particularly seem to control the location of the transition are permeability and consolidation. Permeability is a property of a porous material that represents the ability of fluid to flow through that material (Wang et al., 2019). This paper proposes a material property, namely, consolidation, that represents a material's ability to not collapse during burning and thus remain consolidated. For example, consolidated materials are synthetic polymers and solid wood (embers, timber, and tree trunks), and unconsolidated materials are peat soils and the litter layer made of loose materials such as peat grains, leaves, and needle vegetation. In organic soils, the degree of consolidation depends on the degree of decomposition of parent materials. For example, the presence of partially decomposed hardwood, natural fibers, and tree roots can make organic soils remain consolidated during burning, and once these parent materials are consumed, the organic soils become unconsolidated.

For consolidated materials with high permeability (e.g., PU foam) (**Figure 10A**), the location of the StF transition tends to be initiated within the material (Tse et al., 1996; Bar-Ilan et al., 2005; Putzeys et al., 2007, 2008; Dodd et al., 2012). The high permeability of a material allows oxygen to flow inside the fuel bed. Consolidation of the fuel bed allows the fuel to remain intact as smouldering propagates within the material and forms void spaces. The formation of void spaces is confirmed by the increasing internal permeability of the fuel during smouldering prior to the StF transition (Tse et al., 1996; Putzeys et al., 2007). This void then becomes the favourable space for gaseous fuel to accumulate. The heat produced from the more exothermic char oxidation will ignite the gaseous fuel in the void spaces (**Figure 10A**).

For low permeability and consolidated material (**Figure 10B**). Smouldering propagates at the surface of the material since the oxygen diffusion inside the material is limited. At the surface, the smouldering front also undergoes high convective heat losses. To be self-sustained, smouldering needed to be assisted with decreasing heat loss or external heat flux, i.e., a U-shaped fuel geometry to maximise radiation heat exchange between the smouldering surfaces or deposited embers on fuel bed surface (Ohlemiller, 1991; Manzello et al., 2006b, 2008, 2009, 2012; Manzello and Suzuki, 2014, 2017; Hakes et al., 2018). Under this condition, the transition tends to occur at the surface of the material. Bilbao et al. (2001) conducted an experiment with

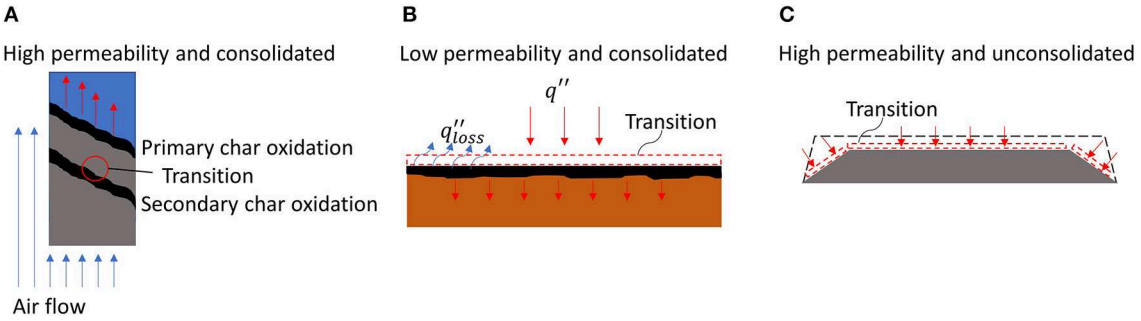

FIGURE 10 | smouldering-to-flaming transition location with respect to permeability and consolidation of the material. **(A)** High permeability and consolidated material, i.e., polyurethane foam, cotton cladding, upholstery material. **(B)** Low permeability and consolidated material, i.e. wood. **(C)** High permeability and unconsolidated material, i.e. dust layer, cellulosic insulation, and organic soil.

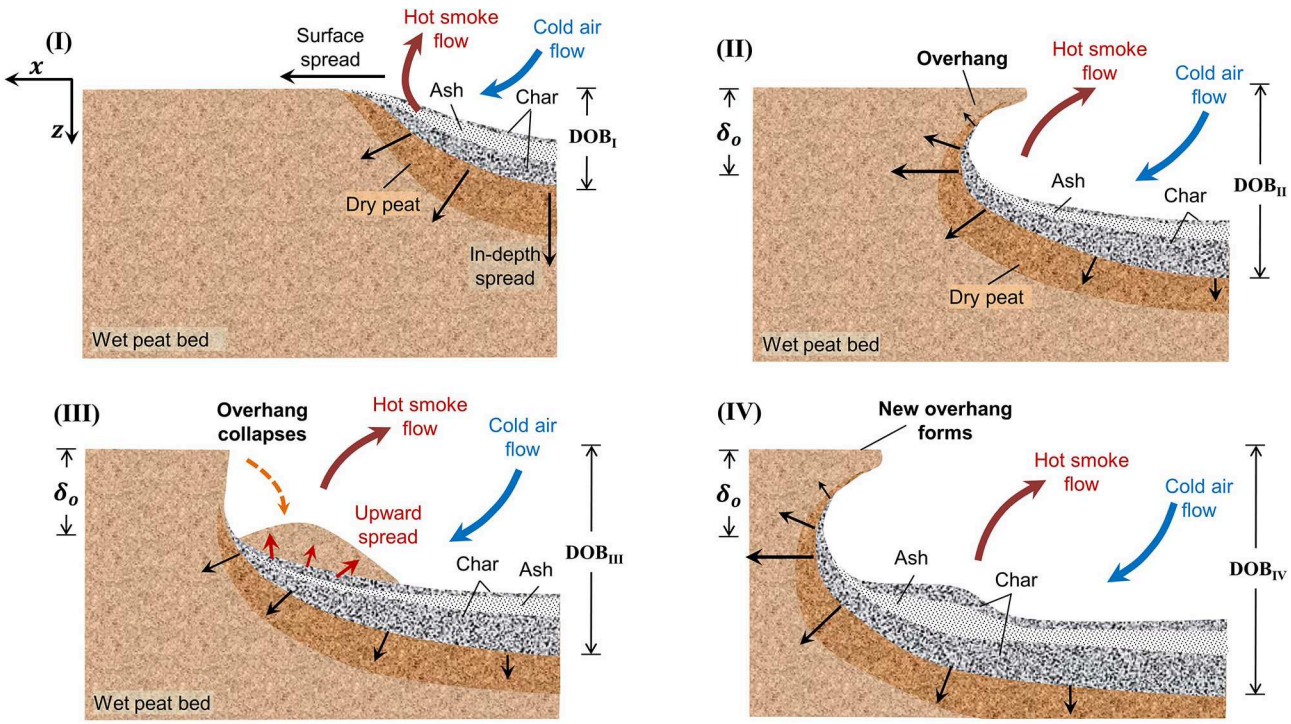

FIGURE 11 | Schematic diagram for the periodic formation and collapse of overhang in smouldering spread over wet peat: **(I)** soon after ignition, **(II)** formation of the overhang, **(III)** collapse and consumption of the overhang, and **(IV)** formation of a new overhang. Illustration from Huang et al. (2016) (X. Huang, CC BY license).

small *P. pinaster* wood, i.e., dimensions of 11 by 11 by 1.9 cm, under radiative heat flux and forced convection. They found that radiative heat flux affected the time to StF transition more than convection did, implying that the low permeability of the material made the smouldering less dependent on airflow and that minimising convective heat losses by assisting smouldering with radiative heat flux governs the StF transition.

In high permeability and unconsolidated materials (**Figure 10C**), the fuel is not able to maintain its structural integrity during burning and thus immediately collapses during fuel consumption. The fuel in this category includes fuel beds made of dusts, cellulosic insulation, vegetation (grasses and pine needles), and organic soils. Most wildland fuels fall in this category, except wood, which is a consolidated fuel with low permeability. In the smouldering of this fuel category, the transition tends to occur at the surface of the fuel bed (Palmer, 1957; Ohlemiller, 1990; Manzello et al., 2006a,b; Valdivieso and Rivera, 2014; Wang et al., 2017; Yang et al., 2018).

For solid fuels that have high permeability and an intermediate degree of consolidation during smouldering, such as peat, an overhang can form and collapse during fire spread (Huang et al., 2016). An overhang is a temporary hanging surface of burning organic soil, where its intermediate layer below has been consumed (**Figure 11**). An overhang is formed because of the

faster horizontal spread rate a few centimeters below the surface due to the reduced convective heat losses compared to the free surface of the organic soil fuel bed (Huang et al., 2016; Rein, 2016). The collapse of the peat overhang is because the char layer is gradually consumed and can no longer support the weight of the above soil. Currently, in the literature, there is no mention of StF transition during overhang formation. However, the possible influence of intermediate consolidation of peat represented by overhang formation and collapse on the StF transition could still be explored since overhang formation and collapse are also recent findings, and their scope of influence on fire dynamics has not yet been identified.

One of the difficulties in mitigating peat fires is its propensity to spread deep below the ground (Page et al., 2002; Rein et al., 2008; Rein, 2016), hence the deep penetration of oxygen diffusion to the smouldering peat. Considering permeability alone, subsurface smouldering propagation can lead to resurfacing of smouldering that can lead to a StF transition. The resurfacing of an underground smouldering front is made possible because of the consolidation of the char layer left behind by oxygen-limited smouldering propagation (Huang and Rein, 2019).

Another parameter found to affect the StF transition, in relation to permeability, is the particle diameter of the fuel bed. For natural fuel beds filled with particles, the permeability is proportional to the square of the particle diameter ($K \sim d_p^2$ $K \sim d_p^2$) (Soulsby, 1997). The particle diameter also affects the heat exchange and mass transfer between the solid matrix and porous pores, thus influencing the chemical reactivity. With increasing particle diameter, the StF transition occurred at a lower critical velocity, which is the velocity at which the StF transition occurs. In smouldering dust beds, the StF transition did not occur when dust particles were <0.1 cm (Palmer, 1957). An increase in particle diameter leads to an increase in the total pore surface area and a decrease in the specific surface area (SSA: total surface area of the fuel bed per unit volume or mass) of the fuel bed. Song et al. (2017) investigated the particle diameter effect on the reaction rate of a heterogeneous coal reaction. Knudsen (intra-particle) diffusion, which is the diffusion of a gas, in this case oxygen, into the interior of particles decreases with increasing particle diameter due to increasing pore surface area or permeability. The decrease in Knudsen diffusion decreases the overall reaction rate of coal oxidation by up to 50%. This finding is contrary to that by Palmer (1957), where increasing particle diameter leads to an increasing tendency for the StF transition. The effects of particle diameter on the Knudsen oxidation rate and StF transition need to be investigated further. Currently, the influence of specific surface area to StF transition cannot be assessed at this point because there are no data available in the literature.

EMBERS AND STF TRANSITION IN WILDFIRES

Embers contribute to the devastating spread of wildfires by being lofted in the fire plume and carried vast distances by strong winds (Pagni, 1993; Butler et al., 1998; Fernandez-Pello, 2017). Embers, commonly called firebrands and different from hot metal fragments, are combustible and rich in carbon. The accumulation of these embers can start local smouldering and, in some cases, exhibit StF transitions that result in fire spread far beyond the original fire front. This behaviour is also known as spotting (**Figure 2**). Field observations of StF are hard to find in the scientific literature, but a few exist. Pagni (1993) qualitatively described the 1991 Oakland Hills wildfire in California, USA, during which embers landed on a downwind region of high fuel load and led to a massive fires conflagration. The report mentions "flaming debris," but we can infer that this term represents a broad range of burning embers, including smouldering embers. This wildfire burned 600 ha, caused 25 fatalities and damaged 2,334 structures (Pagni, 1993). The wind was dry and of high velocity (∼10 m/s), with a strong inversion layer of 600 m, and on a complex hill topography. Field observations of the role of smouldering ember were also recorded in the 1994 South Canyon Fire in Colorado, USA. This fire suddenly shifted from a slow surface fire to a fast crown fire, causing the deaths of 14 firefighters. The surface fire included flaming grass and smouldering litter, with occasional torching of individual trees, which when combined produced flying smouldering embers. This result could imply that the shift from low- to high-intensity fire could have involved the StF transition of smouldering embers. From the survey conducted after the January 1994 wildland fires in Sydney, Australia, 52 of the WUI materials were ignited by embers while the rest, i.e., 18, were ignited by radiation (Babrauskas, 2003). In another investigation, Maranghides and Mell (2009) concluded that 55 of 74 destroyed homes were ignited by embers, 80 min before the arrival of the fire front. This is in agreement with Bell (1985), concluding that radiation alone is rarely the cause of house to be lost.

Manzello et al. (2006a) investigated the ignition of pine straw mulch, shredded hardwood mulch, and cut grass by embers. Fuel MC was either dry or 11% MC and placed inside an aluminum foil pan with dimensions of 23 by 23 by 5.1 cm. The StF transition occurred when four smouldering firebrands 50 mm in diameter were deposited on the samples and exposed to an airflow of 1 m/s. This airflow was lower than the critical velocity of 2 m/s for the StF transition in cellulosic insulation (Ohlemiller, 1990), which may be due to the difference in material or the enhanced radiation feedback between the sample and the firebrands, resulting in more intense smouldering.

To focus the investigation on the ignition of fuel beds, embers can be represented as hot metal particles (Hadden et al., 2011; Wang et al., 2017). This approach eliminates the complexity of the ember reaction process, its variable heat release, and coupled heat transfer interaction between the fuel bed and embers. In addition to these conveniences in investigating fuel bed ignition by hot metal particles, real wildfires are often initiated and accelerated by hot metal particles from clashing power lines and machine processes, such as grinding and welding (Fernandez-Pello, 2017). A smaller particle size leads to a higher temperature required for the flaming ignition of cellulosic fuel beds (Hadden et al., 2011). Particles as small as 19.1 mm with a temperature of 650°C can initiate flaming combustion. Embers with sizes ranging from 25 to 50 mm have been found in studies investigating StF transitions (Manzello et al., 2006a,b, 2008;

Hakes et al., 2018). In pine needle beds, the time to StF transition was ∼2.5–5 min at particle temperatures within the range of smouldering temperatures, ∼630–700°C (Wang et al., 2017). For drier fuel, the StF transition propensity increases, represented by the decreased StF transition time to as short as ∼2 min in fuel with ∼6% MC. In all cases, a larger particle size requires a lower particle temperature to initiate the StF transition in pine needles at higher MC. In comparison, an increasing particle size from 8 to 14 mm at a particle temperature of 925°C placed on a fuel bed at 25% MC can lead from no ignition to the occurrence of a StF transition in pine needle beds. Another interesting finding related to hot metal particle ignition is the effect of the melting process of the metal. It was found that the melting of hot metal particles increases the propensity of smouldering ignition (Urban et al., 2017).

Considering the fire hazard of embers to WUI fuels, Manzello et al. (2008) investigated the showering of firebrands on roofing assemblies. Roofing assemblies were varied into three configurations: (1) valley configuration of only base material, i.e., oriented strand board (OSB); (2) valley configuration of full roofing assembly, i.e., OSB, tar paper, and shingles; and (3) flat configuration of the roofing assembly with gutters filled with dried pine needles and leaves. A StF transition occurred on the (1) valley configuration of only base material and on the (3) flat configuration of the roofing assembly with gutters filled with dried pine needles and leaves. In configuration 1, the StF transition only occurred when the valley configuration was set at a 60° angle. The StF transition occurred due to the accumulation of firebrands in the crevice. The onset of the StF transition was on the back side of the OSB. In this case, the StF transition was due to the chimney effect, as discussed in the section *The Chimney Effect*. The chimney effect was more significant in this case than in the case of upholstered furniture fire due to a smouldering cigarette because the embers continuously accumulated in the crevice. In configuration 3, the StF transition was inside the gutter in the dried pine needles and leaves. The flame did not spread up to the roofing assembly. However, it was able to melt the shingles. It is not discussed whether flaming was preceded by smouldering of the dried pine needles and leaves or went directly to flaming. The time to StF transition was not recorded; however, the experiment was carried out in 6 min, and the StF transition occurred within that time frame. This StF transition time was significantly shorter than the recorded time of the StF transition in the upholstered furniture fire tests due to a smouldering cigarette, i.e., between 20 and 132 min (Clarke and Ottoson, 1976; Bukowski et al., 1977; Harpe et al., 1977; Bukowski, 1979). Extrapolating the scenario of flaming from accumulated vegetation in the gutter, the melted shingles can lead to exposed wood roofing structures. With consistent ember showers lasting longer than 6 min and pre-heated and aged shingles, WUI fires can spread substantially through this mechanism.

The short time to the StF transition in wildland and WUI fuels due to embers certainly shows the scale of wildfire threat, representing sudden fire spread in distant locations. More focused studies closely investigating the mechanism leading to the StF transition of the fuel due to embers are needed. Currently, in the literature, it is not clear whether the StF transition of the fuel is preceded by sustained smouldering of the fuel or only by pyrolysis of the fuel. In the former case, smouldering or flaming embers ignite smouldering of the fuel up to the point where the fuel is self-sustained and spread is uninfluenced by heat from the embers. This self-sustained smouldering later transitions to flaming. In the latter case, the StF transition was piloted ignition of pyrolyzate from the fuel by smouldering embers. Thus, pyrolysis is supported by heat from smouldering embers, and flaming ignition of the fuel occurs in the vicinity of embers where heat is most available. In this case, the StF transition of the embers could also precede flaming ignition of the fuel, where flaming embers act as a heat source for the fuel pyrolysis reaction and pilot ignition of the pyrolyzates from the fuel (Hakes et al., 2018). The comparison of these two cases shows that the embers enhance flaming ignition of the fuel more in the latter case than in the former case, assuming that self-sustained smouldering can take a long time to establish and has equal probability to extinguish as to transition from StF.

Valdivieso and Rivera (2014) investigated the StF transition in self-sustained smouldering of pine needle fuel beds with dimensions of 60 by 15 by 4 cm and, interestingly, they observed that the StF transition is a cyclic transition from smouldering to flaming to smouldering up to the point at which the whole fuel bed is consumed. This cycle occurred with a wind velocity of 1.1 m/s and a fuel MC of 69% (dry mass basis). This cycle was also found in the StF transition of a cellulose fuel bed by Ohlemiller (1990), and was argued to be caused by smouldering fronts that provide heat and pre-heated gaseous fuel. Because the smouldering process is at a lower rate than flaming, the gaseous fuel supply from smouldering fronts soon becomes insufficient to provide self-sustained flaming. In other words, self-sustained flaming could be established if the heat feedback from flaming is sufficient to increase the smouldering rate at a required level of gaseous fuel production. Another way to interpret this cycle is that gaseous fuel is provided by in-depth pyrolysis of fuel. As smouldering progresses, the char layer forms and becomes thick enough to insulate the fuel, decreasing the pyrolyzate diffusion rate to flow outside the fuel bed to mix with oxygen. As smouldering progresses further, the char layer is consumed and becomes thinner. Under this condition, the pyrolyzate diffusion rate increases again and mixes with oxygen. The StF transition occurs once the pyrolyzate/oxygen concentration is above the lower flammability limit. However, whether the StF transition depends on the pyrolysis of unreacted fuel or char or the oxidation of char remains to be determined and could be fuel- and experimental-setup-dependent.

In general, currently there is insufficient statistics and observations of StF transition in field-scale wildfire. These statistics and observations are much-needed data to identify the large gap in the understanding of StF transition and wildfire spread. Largely, rekindle can be initiated by residual smouldering fuel, i.e., wood log, embers, and duff layer, transitioned to flaming, thus starting a new fire front. During the Portugal wildfire in the summer of 2010, rekindle accounted for an additional 2,497 fires (Pacheco et al., 2012). This put a massive burden to firefighters as they need to revisit a reignited fire while under immense pressure to suppress other untreated fires. Pacheco et al. (2012)

discussed the importance of mop-up operation to avoid rekindle. A recent example of rekindle was Canyon Fire 2 in California in October 2017, in which the fire was likely to be started by strong winds pushing smouldering embers from previous fires in late September in the same area (Schwebke, 2017). Rekindle is also an issue when fires survive winter and reignited once weather is warming. This is especially a concern when fires could spread onto organic soils, which is essentially providing a massive amount of fuel supply (Gabbert, 2018). Fires in organic soils have been known to survive under sub-atmospheric oxygen concentration and very wet conditions (Rein, 2016). An example of this is the October 1997 fire in Yeodene peat swamp, Australia. Three weeks after suppression, the fire was thought to be fully extinguished by means of visual observation and infrared signature from aerial operation. However, in March 1998, the fire reignited and burnt 680 ha of the peat swamp area (Gunning, 2019). Due to the unknown cause of the fire, Gunning (2019) also mentioned the possible rekindle of fire in 1881, 1886, 2006, and 2010, emphasising that rekindle possibility can span across years.

CONCLUSIONS

In this paper, 28 studies of StF transition reported in English published from 1957 to 2019 have been reviewed. As shown in **Table 2**, wildland fuels need more attention in terms of their combustion behaviour and StF transition, as only three of the 28 studies observed StF transitions in wildland fuels. By critically reviewing findings in the literature, we identify oxygen supply and heat flux as the primary variables governing the StF transition. Specifically, these two parameters govern the StF transition in fuel subject to external airflow, fuel in a narrow vertical channel configuration, and fuel that undergoes more exothermic SCO. Afterwards, we propose a fuel classification based on the permeability of the fuel and the ability of the fuel to remain consolidated during burning. These two properties of the fuel affect the oxygen supply and heat transfer during fuel combustion, thus affecting the StF transition.

In essence, the StF transition is a spontaneous gas-phase ignition supported by the heat and reaction from smouldering (Tse et al., 1996; Bar-Ilan et al., 2005; Putzeys et al., 2007, 2008; Rein, 2009; Yang et al., 2018). Mechanisms leading to StF transition are governed by complex interactions of heat transfer and chemistry. From studies of widely different experimental setups on samples ranging from 0.1 to 1.2 m (**Table 2**), two variables are found to govern the StF transition, i.e., oxygen supply and heat flux. Airflow has a dual effect on smouldering. Airflow increases the oxygen supply to the fuel, thus increasing the reaction rate of an oxygen-limited spread, which favours the occurrence of the StF transition, but it also increases convective heat losses from the smouldering front, thus decreasing the tendency of the StF transition. The external supply of heat flux minimises heat loss and assists the fuel heating required for self-sustained smouldering progress and pyrolyzate production. Assistive fuel heating can be in the form of external heat flux such as embers in the case of WUI fires or from pertinent features of the fuel configuration such as when heat loss is minimised by the possible presence of radiation exchange between smouldering surfaces, i.e., smouldering at the fuel crevice or smouldering in U-shaped fuels (Alexopoulos and Drysdale, 1988; Ohlemiller, 1991; Ogle and Schumacher, 1998; Manzello et al., 2008, 2009, 2012; Manzello and Suzuki, 2017; Stoliarov et al., 2017; Hakes et al., 2018).

Vertical channel formation in smouldering at a crevice leads to radiation exchange between smouldering char surfaces and the chimney effect, increasing airflow from the buoyant flow (Ogle and Schumacher, 1998; Manzello et al., 2008; Stoliarov et al., 2017). The radiation exchange between smouldering surfaces leads to more effective heating, while buoyant flow increases the oxygen supply to smouldering fronts. The radiation exchange between surfaces minimises the convective cooling effect from the increased buoyant airflow. This mechanism is most relevant to WUI fires (Manzello et al., 2008). The StF transition is favourable at crevice locations in between smouldering fuels, i.e., embers at crevices of wood decks or house roofing, leading to increased buoyant flow through a vertical channel insulated by the char layer, thus minimising heat losses.

Strong char oxidation triggers a StF transition, as it provides heat to accelerate gaseous fuel production from pyrolysis and to ignite gaseous fuel (Torero and Fernandez-Pello, 1995; Tse et al., 1996; Bar-Ilan et al., 2005; Putzeys et al., 2007, 2008; Dodd et al., 2012; Yang et al., 2018). Whether pyrolysis takes place in unreacted fuel or char remains to be determined. SCO represents a sudden increase in the exothermic reaction rate at the smouldering trailing edge and releases more heat than the previous char oxidation at the same location. The role of this strong char oxidation in providing the required gaseous fuel, and regarding its sequentially secondary nature, needs to be further explored in different types of fuel and experimental setups.

Permeability and consolidation of the fuel bed control the location of the StF transition. Both parameters control the propagation of smouldering fronts, ultimately dictating the location of the StF transition (Tse et al., 1996; Putzeys et al., 2007; Dodd et al., 2012). Permeability controls the diffusion of oxygen penetration into the fuel bed, while consolidation controls the availability of space for smouldering to propagate within the fuel bed. Consolidated fuel with high permeability, such as open-celled polyurethane foam, tends to have a transition initiated close to the surface but within the fuel bed. Consolidated fuels with low permeability such as wood and unconsolidated fuels with high permeability such as cellulosic insulation tend to undergo transition at the surface. In a fuel bed such as peat, which is highly permeable and unconsolidated, overhang formation and collapse could alter the StF occurrence due to intermediate production of a char layer that has a tendency to hold its structural integrity but lose it once undergoing further smouldering, leaving only ash.

Deposited embers on a fuel bed increase the propensity of StF due to the embers' role in assisting the fuel heating process. In wildfire propagation, embers contribute to spotting and the quick initiation of new flaming sites (Mell et al., 2010; Caton

et al., 2017; Fernandez-Pello, 2017). The recorded StF transition time from studies of embers deposited on WUI and wildland fuels is <10 min and decreases with drier fuel (Manzello et al., 2008; Wang et al., 2019). With the predicted drier climate in the future, faster and more widespread propagation of WUI fires is to be expected. Considering that population movement contributes to the increase in WUI fire frequency (Mortsch, 2006; Hammer et al., 2007; Tarnocai et al., 2009; Simeoni, 2016) and that current WUI fuels are vulnerable to StF transitions due to embers (Manzello and Suzuki, 2014), more studies should investigate the design of smouldering-resistant material in the WUI area. Fundamentally, this calls for a better understanding of the StF transition mechanism.

This review synthesises the research, identifies regions for further research, and provides information on various StF transition mechanisms in the literature. These mechanisms converge on two fundamental aspects, heat transfer and chemistry. As airflow has a chemical effect (providing oxygen for the exothermic reaction) and a heat transfer effect (convective cooling), vertical channel formation also similarly provides more oxygen (chemistry) from the buoyant effect and a more effective heating process from radiation exchange between smouldering char surfaces (heat transfer). A better understanding of heat transfer and the chemical reactions of the StF transition mechanism can lead to prospective opportunities to better mitigate wildfires and protect the WUI.

AUTHOR CONTRIBUTIONS

MS and GR carried out the literature review. MS, EC, JY, and GR wrote the paper.

FUNDING

The authors would like to thank the European Research Council (ERC) Consolidator Grant HAZE (682587) for research funding and the Doctoral Studies Scholarship funded by the Indonesia Endowment Fund for Education (LPDP).

ACKNOWLEDGMENTS

The authors are grateful for the fruitful discussions with Dr. Haixiang Chen from the University of Science and Technology of China and with Dr. Francesco Restuccia, Dr. Hafiz M. F. Amin, Yuqi Hu, Matthew Bonner, Franz Richter, Dwi M. J. Purnomo, and Benjamin Khoo from Imperial College London.

REFERENCES

Aldushin, A. P., Bayliss, A., and Matkowsky, B. J. (2009). Is there a transition to flaming in reverse smolder waves? *Combust. Flame* 156, 2231–2251. doi: 10.1016/j.combustflame.2009.09.009

Alexopoulos, S., and Drysdale, D. D. (1988). The transition from smouldering to flaming combustion. *Fire Mater.* 13, 37–44. doi: 10.1002/fam.810130106

Babrauskas, V. (2003). *Ignition Handbook: Principles and Applications to Fire Safety Engineering, Fire Investigation, Risk Management and Forensic Science*. Issaquah, WA: Fire Science Pub.

Babrauskas, V. and J. Krasny (1997). Upholstered furniture transition from smoldering to flaming. *J. Forensic Sci.* 42, 1029–1031. doi: 10.1520/JFS14256J

Babrauskas, V., and Krasny, J. F. (1985). *Fire Behavior of Upholstered Furniture*. Washington, DC: National Bureau of Standards; U.S. Department of Commerce.

Bar-Ilan, A., Putzeys, O., Rein, G., and Fernandez-Pello, A. C. (2005). Transition from forward smoldering to flaming in small polyurethane foam samples. *Proc. Combust. Inst.* 30, 2295–2302. doi: 10.1016/j.proci.2004.08.233

Bell, A. (1985). How bushfires set houses alight—lessons from Ash Wednesday. *Ecos* 43, 3–7.

Bilbao, R., Mastral, J. F., Aldea, M. E., Ceamanos, J., Betrán, M., and Lana, J. A. (2001). Experimental and theoretical study of the ignition and smoldering of wood including convective effects. *Combust. Flame* 126, 1363–1372. doi: 10.1016/S0010-2180(01)00251-6

Bukowski, R. W. (1979). *Investigation of the Effects of Heating and Air Conditioning on the Performance of Smoke Detectors in Mobile Homes*. Washington, DC: National Bureau of Standard.

Bukowski, R. W., Christian, W. J., and Waterman, T. E. (1977). *Detector Sensitivity and Siting Requirements for Dwellings*. Boston: National Fire Protection Association.

Butler, B. W., Bartlette, R. A., Bradshaw, L. S., Cohen, J. D., Andrews, P. L., Putnam, T., et al. (1998). *Fire Behavior Associated With the 1994 South Canyon Fire on Storm King Mountain, Colorado*. Ogden, UT: United States Forest Service; Department of Agriculture.

Caton, S. E., Hakes, R. S. P., Gorham, D. J., Zhou, A., and Gollner, M. J. (2017). Review of pathways for building fire spread in the wildland urban interface part I: exposure conditions. *Fire Technol.* 53:429. doi: 10.1007/s10694-016-0589-z

Chang, L., Die, M., Rongkun, P., Bei, P., and Minggao, Y. (2011). "The effect of sample size on smoldering and the transition to flaming combustion," in *2011 Third International Conference on Measuring Technology and Mechatronics Automation*.

Chao, C. Y. H., and Wang, J. H. (2001). Transition from smoldering to flaming combustion of horizontally oriented flexible polyurethane foam with natural convection. *Combust. Flame* 127, 2252–2264. doi: 10.1016/S0010-2180(01)00326-1

Chen, Y., Kauffman, C. W., Sichel, M., Fangrat, J., and Guo, Y. (1990). The transition from smoldering to glowing to flaming combustion. *Chem. Phys. Process. Combust.* 68, 1–4.

Christensen, E., Hu, Y., Restuccia, F., Santoso, M. A., Huang, X., and Rein, G. (2019). "Experimental methods and scales in smouldering wildfires," in *Chapter 17 in Fire Effects in Soil Properties*, eds P. Pereira, J. Mataix-Solera, X. Úbeda, G. Rein, and A. Cerdà (Clayton, VIC: CSIRO), 267–280.

Clarke, F., and Ottoson, J. (1976). Fire death scenarios and fire safety planning. *Fire J.* 70, 20–22.

Dodd, A. B., Lautenberger, C. R, and Fernandez-Pello, C. (2012). Computational modeling of smolder combustion and spontaneous transition to flaming. *Combust. Flame* 159, 448–461. doi: 10.1016/j.combustflame.2011.06.004

Fernandez-Pello, A. C. (2017). Wildland fire spot ignition by sparks and firebrands. *Fire Safety J.* 91, 2–10. doi: 10.1016/j.firesaf.2017.04.040

Frandsen, W. H. (1987). The influence of moisture and mineral soil on the combustion limits of smoldering forest duff. *Canad. J. Forest Res.* 17, 1540–1544

Frandsen, W. H. (1997). Ignition probability of organic soils. *Canad. J. Forest Res.* 27, 1471–1477.

Gabbert, B. (2018). Overwintering fires are a concern in Northern Rockies. *Wildfire Today*. Available online at: https://wildfiretoday.com/2018/05/12/overwintering-fires-are-a-concern-in-northern-rockies/ (cited June 11, 2019).

Gunning, M. (2019). "Managing the complexities and consequences of peat fires around communities," in *Proceedings for the 6th International Fire Behavior and Fuels Conference* (Missoula, MT: International Association of Wildland Fire).

Hadden, R., Alkatib, A., Rein, G., and Torero, J. L. (2014). Radiant ignition of polyurethane foam: the effect of sample size. *Fire Technol.* 50, 673–691. doi: 10.1007/s10694-012-0257-x

Hadden, R., and Rein, G. (2011). "Burning and water suppression of smoldering coal fires in small-scale laboratory experiments," in *Coal and Peat Fires: A Global Perspective*, eds G. B. Stracher, A. Prakash, and E. V. Sokol (Oxford), 317–326. doi: 10.1016/B978-0-444-52858-2.00018-9

Hadden, R. M., Scott, S., Lautenberger, C., and Fernandez-Pello, A.C. (2011). Ignition of combustible fuel beds by hot particles: An experimental and theoretical study. *Fire Technol.* 47, 341–355. doi: 10.1007/s10694-010-0181-x

Hagen, B. C., Frette, V., Kleppe, G., and Arntzen, B. J. (2015). Transition from smoldering to flaming fire in short cotton samples with asymmetrical boundary conditions. *Fire Safety J.* 71, 69–78. doi: 10.1016/j.firesaf.2014.11.004

Hakes, R. S. P., Salehizadeh, H., Weston-Dawkes, M. J., and Gollner, M. J. (2018). Thermal characterization of firebrand piles. *Fire Safety J.* 104, 34–42. doi: 10.1016/j.firesaf.2018.10.002

Hammer, R., Radeloff, V., Fried, J., and Stewart, S. (2007). Wildland–urban interface housing growth during the 1990 in California, Oregon, and Washington. *Int. J. Wildland Fire* 16, 255–265. doi: 10.1071/WF05077

Harpe, S. W., Waterman, T. E., and Christian, W. J. (1977). *Detector Sensitivity and Siting Requirements for Dwellings, Phase 2*. Boston: National Fire Protection Association.

Hu, Y., Christensen, E., Restuccia, F., and Rein, G. (2019). Transient gas and particle emissions from smouldering combustion of peat. *Proc. Combust. Inst.* 37, 4035–4042. doi: 10.1016/j.proci.2018.06.008

Hu, Y., Fernandez-Anez, N., Smith, T. E. L., and Rein, G. (2018). Review of emissions from smouldering peat fires and their contribution to regional haze episodes. *Int. J. Wildland Fire* 27, 293–312. doi: 10.1071/WF17084

Huang, X., and Rein, G. (2014). Smouldering combustion of peat in wildfires: inverse modelling of the drying and the thermal and oxidative decomposition kinetics. *Combust. Flame* 161, 1633–1644. doi: 10.1016/j.combustflame.2013.12.013

Huang, X., and Rein, G. (2017). Downward spread of smouldering peat fire: the role of moisture, density and oxygen supply. *Int. J. Wildland Fire* 26, 907–918. doi: 10.1071/WF16198

Huang, X., and Rein, G. (2019). Upward-and-downward spread of smoldering peat fire. *Proc. Combust. Inst.* 37, 4025–4033. doi: 10.1016/j.proci.2018.05.125

Huang, X., Restuccia, F., Gramola, M., and Rein, G. (2016). Experimental study of the formation and collapse of an overhang in the lateral spread of smouldering peat fires. *Combust. Flame* 168, 393–402. doi: 10.1016/j.combustflame.2016.01.017

Huijnen, V., Wooster, M. J., Kaiser, J. W., Gaveau, D. L., Flemming, J., Parrington, M., et al. (2016). Fire carbon emissions over maritime southeast Asia in 2015 largest since 1997. *Sci. Rep.* 6:26886. doi: 10.1038/srep26886

Lin, S., Sun, P., and Huang X. (2019). Can peat soil support a flaming wildfire? *Int. J. Wildland Fire* 28, 601–613. doi: 10.1071/WF19018

Manzello, S., Cleary, T. G., Shields, J. R., and Yang, J. C. (2006a). Ignition of mulch and grasses by firebrands in wildland-urban interface fires. *Int. J. Wildland Fire* 15, 427–431. doi: 10.1071/WF06031

Manzello, S., Cleary, T. G., Shields, J. R., and Yang, J. C. (2006b). On the ignition of fuel beds by firebrands. *Fire Mater.* 30, 77–87. doi: 10.1002/fam.901

Manzello, S., Shields, J., Hayashi, Y., and Nii, D. (2008). Investigating the vulnerabilities of structures to ignition from a firebrand attack. *Fire Safety Sci.* 9, 143–154. doi: 10.3801/iafss.fss.9-143

Manzello, S. L. (2014). Enabling the investigation of structure vulnerabilities to wind-driven firebrand showers in wildland urban interface (WUI) fires. *Fire Safety Sci.* 11, 83–96. doi: 10.3801/IAFSS.FSS.11-83

Manzello, S. L., Almand, K., Guillaume, E., Vallerent, S., Hameury, S., and Hakkarainen, T. (2018). FORUM position paper, the growing global wildland urban interface (WUI) fire dilemma: Priority needs for research. *Fire Safety J.* 100, 64–66. doi: 10.1016/j.firesaf.2018.07.003

Manzello, S. L., Park, S. –H., and Cleary, T. G. (2009). Investigation on the ability of glowing firebrands deposited within crevices to ignite common building materials. *Fire Safety J.* 44, 894–900. doi: 10.1016/j.firesaf.2009.05.001

Manzello, S. L., and Quarles, S. L. (2017). Special section on structure ignition in wildland–urban interface (WUI) fires. *Fire Technol.* 53, 425–427. doi: 10.1007/s10694-016-0639-6

Manzello, S. L., and Suzuki, S. (2014). Exposing decking assemblies to continuous wind-driven firebrand showers. *Fire Safety Sci.* 11, 1339–1352. doi: 10.3801/IAFSS.FSS.11-1339

Manzello, S. L., and Suzuki, S. (2017). Experimental investigation of wood decking assemblies exposed to firebrand showers. *Fire Safety J.* 92, 122–131. doi: 10.1016/j.firesaf.2017.05.019

Manzello, S. L., Suzuki, S., and Hayashi, Y. (2012). Enabling the study of structure vulnerabilities to ignition from wind driven firebrand showers: a summary of experimental results. *Fire Safety J.* 54, 181–196. doi: 10.1016/j.firesaf.2012.06.012

Manzello, S. L., Suzuki, S., and Nii, D. (2017). Full-scale experimental investigation to quantify building component ignition vulnerability from mulch beds attacked by firebrand showers. *Fire Technol.* 53, 535–551. doi: 10.1007/s10694-015-0537-3

Maranghides, A., and Mell, W. (2009). *A Case Study of a Community Affected by the Witch and Guejito Fires*. Gaithersburg, MD: National Institute of Science and Technology. NIST Technical Note 1635.

Mell, W., Manzello, S., Maranghides, A., Butry, D., and Rehm, R. (2010). The wildland-urban interface fire problem—Current approaches and research needs. *Int. J. Wildland Fire* 19, 238–251. doi: 10.1071/WF07131

Mortsch, L. D. (2006). "Impact of climate change on agriculture, forestry and wetlands," in *Climate Change and Managed Ecosystems*, eds. J. Bhatti, R. Lal, M. Apps, and M. Price (Boca Raton, FL: Taylor & Francis; CRC Press), 45–67.

NWCG (2012). *Glossary of Wildland Fire Terminology*. Available online at: http://www.nwcg.gov/pms/pubs/glossary/ (archived by WebCite® at http://www.webcitation.org/65wjoO4i7) (accessed on March 5, 2012).

Ogle, R. A., and Schumacher, J. L. (1998). Fire patterns on upholstered furniture: Smoldering versus flaming combustion. *Fire Technol.* 34, 247–265. doi: 10.1023/a:1015397907280

Ohlemiller, T. J. (1985). Modeling of smoldering combustion propagation. *Progr. Energy Combust. Sci.* 11, 277–310. doi: 10.1016/0360-1285(85)90004-8

Ohlemiller, T. J. (1990). Forced smolder propagation and the transition to flaming in cellulosic insulation. *Combust. Flame* 81, 354–365. doi: 10.1016/0010-2180(90)90031-L

Ohlemiller, T. J. (1991). Smoldering combustion propagation on solid wood. *Fire Safety Sci.* 3, 565–574. doi: 10.3801/IAFSS.FSS.3-565

Ortiz-Molina, M. G., Toong, T.-Y., Albert Moussa, N., and Tesoro, G. C. (1979). Smoldering combustion of flexible polyurethane foams and its transition to flaming or extinguishment. *Symp. Combust.* 17, 1191–1200. doi: 10.1016/S0082-0784(79)80113-7

Pacheco, A. P., Claro, J., and Oliveira, T. (2012). "Rekindle dynamics: Validating the pressure on wildland fire suppression resources and implications for fire management in Portugal," in *Modelling, Monitoring, and Management of Forest Fires III*, eds. C. A. Brebbia and G. Perona (Southampton: WIT Press), 225–236.

Page, S. E., Siegert, F., Rieley, J. O., Boehm, H. D., Jaya, A., and Limin, S. (2002). The amount of carbon released from peat and forest fires in Indonesia during 1997. *Nature* 420:61. doi: 10.1038/nature01131

Pagni, P. J. (1993). Causes of the 20 October 1991 Oakland Hills conflagration. *Fire Safety J.* 21, 331–339.

Palmer, K. N. (1957). Smouldering combustion in dusts and fibrous materials. *Combust. Flame* 1, 129–154. doi: 10.1016/0010-2180(57)90041-X

Putzeys, O., Bar-Ilan, A., Rein, G., Fernandez-Pello, A. C., and Urban, D. L. (2007). The role of secondary char oxidation in the transition from smoldering to flaming. *Proc. Combust. Inst.* 31, 2669–2676. doi: 10.1016/j.proci.2006.08.006

Putzeys, O. M., Carlos Fernandez-Pello, A., and Urban, D (2006). Ignition of combustion modified polyurethane foam. *J. ASTM Int.* 3, 1–11. doi: 10.1520/JAI13558

Putzeys, O. M., Fernandez-Pello, A. C., Rein, G., and Urban, D. L. (2008). The piloted transition to flaming in smoldering fire retarded and non-fire retarded polyurethane foam. *Fire Mater.* 32, 485–499. doi: 10.1002/fam.981

Ramadhan, M. L., Palamba, P., Ali, I., Fahri, K., Engkos, A., and Nugroho, Y. S. (2017). Experimental study of the effect of water spray on the spread of smoldering in Indonesian peat fires. *Fire Safety J.* 91, 671–679. doi: 10.1016/j.firesaf.2017.04.012

Ratnasari, N. G., Dianti, A., Pither, P., Ramadhan, M. L., Prayogo, G., Sunjarianto, P. A., et al. (2018). Laboratory scale experimental study of foam suppression on smouldering combustion of a tropical peat. *J. Phys.* 1107:052003. doi: 10.1088/1742-6596/1107/5/052003

Rein, G. (2009). Smouldering combustion phenomena in science and technology. *Int. Rev. Chem. Eng.* 1, 3–18. Available online at: https://www.era.lib.ed.ac.uk/handle/1842/2678

Rein, G. (2013). "Smouldering fires and natural fuels," in *Fire Phenomena and the Earth System: An Interdisciplinary Guide to Fire Science*, ed. C. M. Belcher (West Sussex: John Wiley & Sons, Ltd.), 15–33.

Rein, G. (2016). "Smoldering combustion," in *SFPE Handbook of Fire Protection Engineering*, eds M. J. Hurley, D. Gottuk, J. R. Hall, K. Harada, E. Kuligowski, M. Puchovsky, J. Torero, J. M. Watts, and C. Wieczoreks (New York, NY: Springer New York), 581–603.

Rein, G., Carlos Fernandez-Pello, A., and Urban, D. L. (2007). Computational model of forward and opposed smoldering combustion in microgravity. *Proc. Combust. Inst.* 31, 2677–2684. doi: 10.1016/j.proci.2006.08.047

Rein, G., Cleaver, N., Ashton, C., Pironi, P., and Torero, J. (2008). The severity of smouldering peat fires and damage to the forest soil. *Catena* 74, 304–309. doi: 10.1016/j.catena.2008.05.008

Santoso, M. A., Huang, X., Prat-Guitart, N., Christensen, E., Hu, Y., and Rein, G. (2019). "Smouldering fires and soils, Chapter 13," in *Fire effects in soil properties*, ed P. Pereira (Clayton, VIC: CSIRO), 203–216.

Sato, K., and Sega, S. (1991). Mode of burning zone spread in an opposed gas flow. *Combust. Flame* 83, 146–154. doi: 10.1016/0010-2180(91)90209-T

Schwebke, S. (2017). *Canyon Fire 2, Which Torched 9,200-Plus Acres and Destroyed Homes, Ignited by Embers From Previous Fire*. Available from: https://www.ocregister.com/2017/11/06/canyon-fire-2-which-torched-9000-plus-acres-and-destroyed-homes-ignited-by-embers-from-previous-fire/ss (accessed June 11, 2019).

Simeoni, A. (2016). "Wildland fires," in *SFPE Handbook of Fire Protection Engineering*, eds. M. J. Hurley, D. Gottuk, J. R. Hall, K. Harada, E. Kuligowski, M. Puchovsky, J. Torero, J. M. Watts, and C. Wieczorek (New York, NY: Springer New York), 3283–3302.

Song, Z., Huang, X., Luo, M., Gong, J., and Pan, X. (2017). Experimental study on the diffusion-kinetics interaction in heterogeneous reaction of coal. *J. Thermal Anal. Calorim.* 129, 1625–1637. doi: 10.1007/s10973-017-6386-1

Soulsby, R. (1997). *Dynamics of Marine Sands: A Manual for Practical Applications.* London: Thomas Telford.

Stoliarov, S. I., Zeller, O., Morgan, A. B., and Levchik, S. (2017). An experimental setup for observation of smoldering-to-flaming transition on flexible foam/fabric assemblies. *Fire Mater.* 42, 128–133. doi: 10.1002/fam.2464

Suzuki, S., Manzello, S. L., Kagiya, K., Suzuki, J., and Hayashi, Y. (2015). Ignition of mulch beds exposed to continuous wind driven firebrand showers. *Fire Technol.* 51, 905–922. doi: 10.1007/s10694-014-0425-2

Tarnocai, C., Canadell, J. G., Schuur, E. A. G., Kuhry, P., Mazhitova, G., and Zimov, S. (2009). Soil organic carbon pools in the northern circumpolar permafrost region. *Global Biogeochem. Cycles* 23, 1–11. doi: 10.1029/2008GB003327

Torero, J. L., and Fernandez-Pello, A. C. (1995). Natural convection smolder of polyurethane foam, upward propagation. *Fire Safety J.* 24, 35–52. doi: 10.1016/0379-7112(94)00030-J

Tse, S. D., Fernandez-Pello, C. A., and Miyasaka, K. (1996). Controlling mechanisms in the transition from smoldering to flaming of flexible polyurethane foam. *Symp. Combust.* 26, 1505–1513. doi: 10.1016/S0082-0784(96)80372-9

Urban, J. L., Zak, C. D., Song, J., and Fernandez-Pello, C. (2017). Smoldering spot ignition of natural fuels by a hot metal particle. *Proc. Combust. Inst.* 36, 3211–3218. doi: 10.1016/j.proci.2016.09.014

Valdivieso, J. P., and Rivera, J. (2014). Effect of wind on smoldering combustion limits of moist pine needle beds. *Fire Technol.* 50, 1589–1605. doi: 10.1007/s10694-013-0357-2

Wang, F., Jiao, L., Lian, P., and Zeng, J. (2019). Apparent gas permeability, intrinsic permeability and liquid permeability of fractal porous media: carbonate rock study with experiments and mathematical modelling. *J. Pet. Sci. Eng.* 173, 1304–1315. doi: 10.1016/j.petrol.2018.10.095

Wang, S., Huang, X., Chen, H., and Liu, N. (2017). Interaction between flaming and smouldering in hot-particle ignition of forest fuels and effects of moisture and wind. *Int. J. Wildland Fire* 26, 71–81. doi: 10.1071/WF16096

World Health Organization (2006). *Air Quality Guidelines: Global Update 2005: Particulate Matter, Ozone, Nitrogen Dioxide, and Sulfur Dioxide*. Copenhagen: World Health Organization.

Yang, J., Liu, N., Chen, H., and Gao, W. (2018). Smoldering and spontaneous transition to flaming over horizontal cellulosic insulation. *Proc. Combus. Inst.* 37, 4073–4081. doi: 10.1016/j.proci.2018.05.054

Zhou, K., Suzuki, S., and Manzello, S. L. (2015). Experimental study of firebrand transport. *Fire Technol.* 51, 785–799. doi: 10.1007/s10694-014-0411-8

Conflict of Interest Statement: The authors declare that the research was conducted in the absence of any commercial or financial relationships that could be construed as a potential conflict of interest.